

AEDC-TR-68-197

ay!

**ARCHIVE COPY
DO NOT LOAN**



**EXPERIMENTAL INVESTIGATION OF TWO BLUNT
TRAILING EDGE SUPERSONIC COMPRESSOR ROTORS
OF DIFFERENT BLADE THICKNESSES AND WITH
CIRCULAR ARC CAMBER LINE**

**C. T. Carman and J. R. Myers
ARO, Inc.
and**

**A. J. Wennerstrom and John W. Steurer
Aerospace Research Laboratories**

September 1968

This document has been approved for public release
and sale; its distribution is unlimited.

**ENGINEERING SUPPORT FACILITY
ARNOLD ENGINEERING DEVELOPMENT CENTER
AIR FORCE SYSTEMS COMMAND
ARNOLD AIR FORCE STATION, TENNESSEE**

AEDC TECHNICAL LIBRARY



6609 1E000 0220 5

PROPERTY OF U. S. AIR FORCE
AEDC LIBRARY
F40600 - 69 - C - 0001

NOTICES

When U. S. Government drawings specifications, or other data are used for any purpose other than a definitely related Government procurement operation, the Government thereby incurs no responsibility nor any obligation whatsoever, and the fact that the Government may have formulated, furnished, or in any way supplied the said drawings, specifications, or other data, is not to be regarded by implication or otherwise, or in any manner licensing the holder or any other person or corporation, or conveying any rights or permission to manufacture, use, or sell any patented invention that may in any way be related thereto.

Qualified users may obtain copies of this report from the Defense Documentation Center.

References to named commercial products in this report are not to be considered in any sense as an endorsement of the product by the United States Air Force or the Government.

ERRATA

AEDC-TR-68-197, September 1968

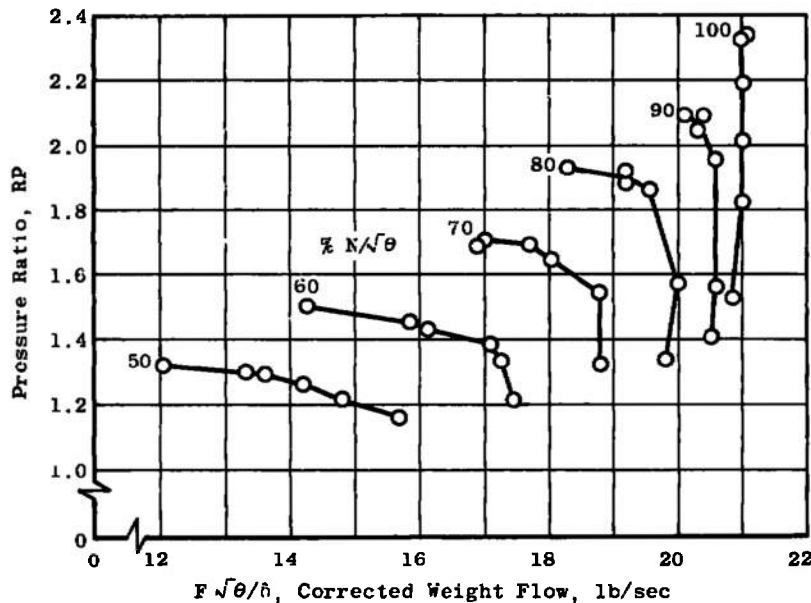
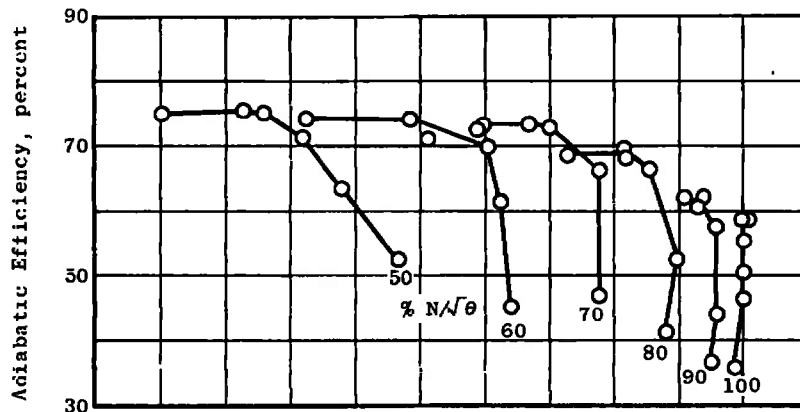
EXPERIMENTAL INVESTIGATION OF TWO BLUNT TRAILING EDGE SUPERSONIC COMPRESSOR ROTORS OF DIFFERENT BLADE THICKNESSES AND WITH CIRCULAR ARC CAMBER LINE

C. T. Carman and J. R. Myers, ARO, Inc.
A. J. Wennerstrom and John W. Steurer, Aerospace Research Laboratories

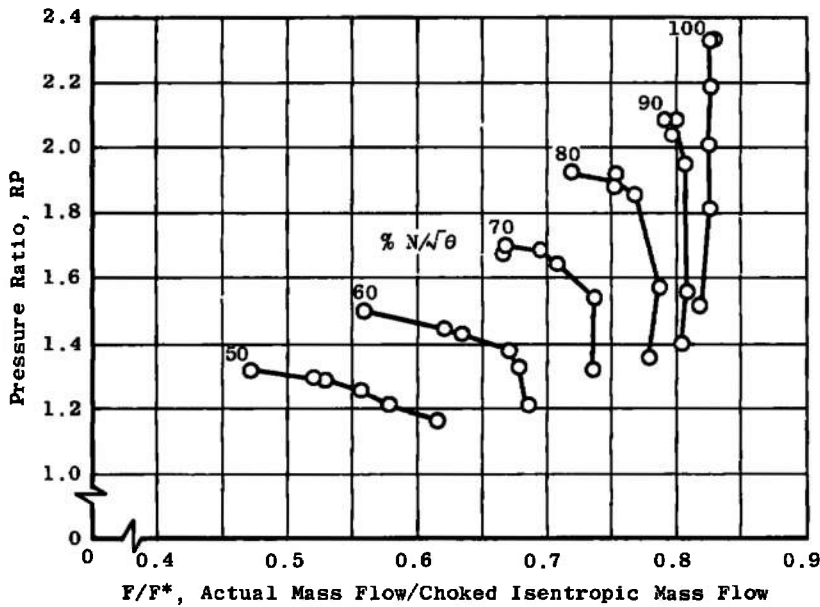
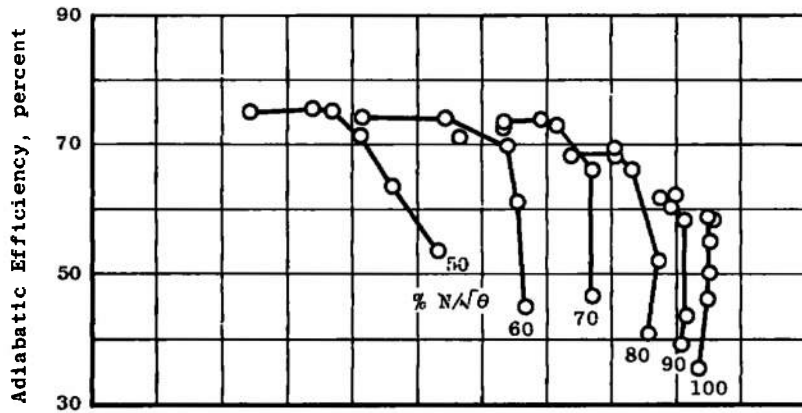
Arnold Engineering Development Center
Air Force Systems Command
Arnold Air Force Station, Tennessee

Please substitute these Figs. IV-1a and b for those on pages 30 and 31 in subject report.

AEDC-TR-68-197



o. Compressor Performance Characteristics Based on Equivalent Weight Flow
Fig. IV-1 Configuration 1



b. Compressor Performance Characteristics Based on Weight Flow Ratio

Fig. IV-1 Continued

EXPERIMENTAL INVESTIGATION OF TWO BLUNT
TRAILING EDGE SUPERSONIC COMPRESSOR ROTORS
OF DIFFERENT BLADE THICKNESSES AND WITH
CIRCULAR ARC CAMBER LINE

C. T. Carman and J. R. Myers
ARO, Inc.

and

A. J. Wennerstrom and John W. Steurer
Aerospace Research Laboratories

This document has been approved for public release
and sale; its distribution is unlimited.

FOREWORD

This report was prepared by Messrs. C. T. Carman and J. R. Myers of ARO, Inc. (a subsidiary of Sverdrup & Parcel and Associates, Inc.), contract operator of the Arnold Engineering Development Center (AEDC), Air Force Systems Command (AFSC), Arnold Air Force Station, Tennessee, and Dr. Arthur J. Wennerstrom and 1st Lt John W. Steurer of the Fluid Dynamics Facilities Research Laboratory of the Aerospace Research Laboratories, OAR, Wright-Patterson Air Force Base, Ohio.

Aerodynamic design and analysis of the compressor rotors were conducted at the Aerospace Research Laboratories. Mechanical design and all experimental work were conducted at the Arnold Engineering Development Center. The complete program was sponsored by the Aerospace Research Laboratories under Program Element 6144501F, Project 7065, "Aerospace Simulation Techniques Research," under the direction of Mr. Elmer G. Johnson. The work was performed between August 1965 and January 1967. The report was submitted for publication on August 12, 1968.

This technical report has been reviewed and is approved.

Hans K. Doetsch
Technical Advisor
Directorate of Plans
and Technology

Edward R. Feicht
Colonel, USAF
Director of Plans
and Technology

ABSTRACT

Two configurations of blunt-trailing-edge supersonic compressor blades were tested with air in the AEDC compressor rig. The performance of these blades was investigated over the speed range from 50 to 100 percent of design speed. The performance of the two blade configurations is compared, and the effect of the modifications between the two configurations is evaluated.

CONTENTS

| | <u>Page</u> |
|--------------------------------------|-------------|
| ABSTRACT | iii |
| NOMENCLATURE | vi |
| I. INTRODUCTION | 1 |
| II. APPARATUS | 2 |
| III. PROCEDURE | 4 |
| IV. RESULTS AND DISCUSSION | 4 |
| V. CONCLUSIONS | 7 |
| REFERENCES | 7 |

APPENDIXES

I. ILLUSTRATIONS

Figure

| | |
|---|----|
| 1. Blade Geometry of Mean Radius Profile | 11 |
| 2. Cross-Sectional View of Experimental Compressor | 13 |
| 3. Details of Instrumentation Stations | 14 |
| 4. Rotor Isentropic Efficiency. | 17 |
| 5. Rotor Total Pressure Ratio | 17 |
| 6. Casing Static Pressure Distribution at Design Speed and Maximum Back Pressure. | 18 |
| 7. Efficiency Distribution at Design Speed and Maximum Back Pressure | 19 |
| 8. Total Pressure Distribution at Design Speed and Maximum Back Pressure. | 19 |
| 9. Corrected Enthalpy Rise at Design Speed and Maximum Back Pressure | 20 |
| 10. Specific Mass Flow Distribution at Design Speed and Maximum Back Pressure. | 20 |
| 11. Absolute Exit Mach Number Distribution at Design Speed and Maximum Back Pressure | 21 |
| 12. Absolute Exit Flow Angle Distribution at Design Speed and Maximum Back Pressure | 21 |

| | <u>Page</u> |
|--|-------------|
| II. METHODS OF CALCULATION | 22 |
| III. MEASUREMENT UNCERTAINTY | 25 |
| IV. DATA SUMMARY FOR CONFIGURATIONS 1 AND 2. | 29 |

NOMENCLATURE

| | |
|----------------|--|
| A | Area, in. ² |
| C | Absolute velocity, ft/sec |
| C _f | Flow coefficient |
| C _p | Specific heat at constant pressure |
| d | Axial distance from blade leading edge, in. |
| F | Weight flow, lb/sec |
| G | Specific weight flow, lb/sec-in. ² |
| g | Local acceleration of gravity, 32.14 ft/sec ² |
| H | Enthalpy |
| IW | Inner wall of compressor annulus |
| J | Mechanical equivalent of heat, 778.3 ft-lb/Btu |
| M | Mach number |
| N | Rotational speed, rpm |
| OW | Outer wall of compressor annulus |
| P | Total pressure, psia |
| p | Static pressure, psia |
| R | Gas constant for air, 53.34 ft-lb/lb°R |
| Re | Reynolds number |
| RF | Thermocouple impact-recovery factor |

| | |
|-----------------|--|
| RP | Pressure ratio |
| r | Radius, in. |
| T | Total temperature, °R |
| t | Static temperature, °R |
| U | Circumferential blade velocity, ft/sec |
| W | Relative velocity, ft/sec |
| α | Absolute flow angle relative to axis of rotation, deg |
| β | Relative flow angle |
| γ | Ratio of specific heats |
| δ | Ratio of inlet total pressure to the ARDC model sea-level atmosphere (14.7 psia) |
| $\sqrt{\theta}$ | Ratio of inlet absolute total temperature to absolute total temperature of ARDC model sea-level atmosphere (519.3°R) |

SUBSCRIPTS

| | |
|------------|-------------------------------------|
| 0, 1, 2, 3 | Compressor instrumentation stations |
| a | Adiabatic |
| av | Average |
| calc | Calculated |
| deg | Degrees |
| i | Indicated |
| isen | Isentropic |
| w | Relative |

SECTION I INTRODUCTION

This is the first of a series of reports which present detailed experimental data from the supersonic compressor research program of the Aerospace Research Laboratories. The experimental portion of this program is being conducted at the Arnold Engineering Development Center. To date, the program has only considered rotors of relatively high solidity which employ blades having blunt trailing edges; i.e., the maximum blade thickness is at 100 percent chord. This design concept was first proposed in Ref. 1. The blading is designed so that the flow passages have relatively constant area and, as a result of camber, the trailing edges remain blunt. The geometry is arranged with a suitable passage length-to-width ratio in such a way that a pseudo-shock diffusion is encouraged between blades. The flow at the trailing edges is allowed to undergo a sudden-area-increase diffusion process which is reasonably efficient if the trailing edge Mach number is not close to unity. A complete discussion of the design philosophy is given in Ref. 2.

Limited testing of the 5-in. rotor described in Ref. 1 provided some encouraging results. Therefore, the initial tests of the current 22-in.-diam rotor were undertaken to evaluate the proposed design concepts.

The overall performance of the first configuration tested was discussed and compared with a theoretical analysis in Ref. 3. In general, the performance was poor. The maximum pressure ratio attained was 2.34 at an adiabatic efficiency of only 59 percent. However, the theoretical analysis suggested that this performance could be improved by incorporating the following modifications: (1) a reduction in the blade trailing-edge thickness, (2) a redistribution of the blade camber, and (3) annulus contouring.

The purpose of this series of reports is twofold: First, to present the complete set of data for the configurations tested; secondly, to present the data in a manner which allows the merits of the above modifications to be evaluated. This report specifically deals with the effects of reducing the blade trailing-edge thickness or, preferably, the blade thickness-to-spacing ratio (t/s). Subsequent reports will deal with the other suggested modifications.

Data from two rotors are presented and compared in this report. Both rotors employ circular arc blade surfaces. The rotors differ only in the blade thickness at the trailing edge and, as a consequence, in the amount of divergence in passage area which occurs through the blade row. All other characteristics are identical. The increased passage divergence was achieved by generating new circular arc surfaces around the camber line of the first rotor in a manner which reduced the blade thickness.

SECTION II APPARATUS

2.1 COMPRESSOR DESIGN

The rotor configurations described in this report were designed to provide a direct continuation of the work reported in Ref. 1; however, the configurations were of larger scale than those discussed in Ref. 1 so that more detailed and accurate measurements could be taken. Therefore, no new thinking was applied to the basic aerodynamic design of the rotors reported herein. A mid-radius inlet blade angle of 60 deg (from axial) and a mid-radius exit blade angle of 30 deg were employed, resulting in a camber of 30 deg, as before. Because the design philosophy intended to employ a pseudo-shock diffusion process, a solidity of 3.0 was chosen to provide a relatively high passage length-to-width ratio. It was hoped to achieve a total pressure ratio of approximately 3.0 at a corrected tip speed of 1600 ft/sec. The mean-radius relative inlet Mach number at design speed and zero incidence would be 1.7.

The hub/tip radius ratio for these tests was 0.9, and the rotor tip diameter was 22 in. The high hub/tip ratio was chosen in order to minimize inviscid three-dimensional flow effects. No hub or tip contouring was employed for the configurations presented in this report.

The blade surfaces at mid-radius were circular arcs extending from a small leading-edge radius to a point of maximum thickness at the trailing edge. The surfaces were symmetrical with respect to a circular arc camber line. Since the trailing edges end abruptly in sharp corners, the blades have the appearance of thin, curved wedges. The blade surfaces between hub and tip are formed by geometric spirals passing through the circular arcs at mid-radius. That is to say, a line passing through, and normal to, the compressor axis and which is moved through the outline of a mid-radius blade element will generate the blade surface from hub to tip. Thus, the pitch of the spiral surfaces is radially constant but axially variable. As a result, the blades are slightly thicker at the tip than at the root.

Because of the high solidity and relatively short chord length, 126 blades were required. Since blade attachment would have been excessively expensive, the blading was machined directly into the rim of the wheel.

The geometry of the first configuration at mid-radius is presented in Fig. 1a. Minimum flow area between blades occurs on a surface extending from the base of the leading-edge radius of one blade to the nearest point on the suction surface of an adjacent blade. In the confined portion of the flow passage, this area increases approximately 10 percent from entrance to exit. A parameter which has proven useful for performance

calculations with blunt trailing-edge blades (see Ref. 3) is the ratio of trailing-edge thickness to blade spacing, measured circumferentially. The thickness-to-spacing ratio for this first rotor was 0.395.

The geometry of the second configuration at mid-radius is presented in Fig. 1b. This differs from the first in that the thickness-to-spacing ratio has been reduced to 0.272, resulting in a larger increase in flow area between the passage entrance and exit. For this configuration the area increases approximately 27 percent. Theoretical calculations presented in Ref. 3 indicated that increased passage divergence should lead to an increase in performance, if boundary-layer blockage does not significantly increase. The particular value of 0.272 was chosen in order to enable comparison with data presented in Ref. 4 for a similar configuration.

2.2 COMPRESSOR RIG

Since complete details on the compressor rig are presented in Ref. 5, only a limited description is provided here. A cross section of the compressor is shown in Fig. 2. The incoming air is drawn from a large settling chamber containing a straightener and screens. The inner wall of the outer casing is completely cylindrical throughout the entire central section of the compressor, and the hub wall is also cylindrical downstream of the compressor. However, the base of the bulletnose which extends into the central section of the compressor is a 1.0-deg. cone to provide a slight flow acceleration all the way to the rotor leading-edge plane. The discharging flow enters a radial diffusing section which terminates in a circumferential throttle valve. The throttle valve has a series of equally spaced and sized discharge ports around the periphery to eliminate as much as possible any asymmetric conditions which might feed back to the compressor. No stator blade rows were used in conjunction with these experiments. The test rig is a closed-loop system, incorporating a heat exchanger and a venturi to measure mass flow in the return loop. Inlet total pressure and temperature were maintained at approximately standard atmospheric conditions, and all presented data are corrected to standard conditions.

2.3 INSTRUMENTATION

Aerodynamic pressures and/or temperatures are measured at the stations shown in Fig. 2. Axial and radial locations and details of the measuring stations in the compressor and venturi are shown in Fig. 3.

Total pressure and total temperature upstream of the rotor were measured with pairs of 5-element rakes placed 1.0 in. ahead of the rotor. These pressure probes were simple impact tubes since the flow direction is uniform and known. The temperature probes contain iron-constantan thermocouples in diffuser shrouds. The probe elements were centered at the centroids of circumferential bands of equal flow area. Total pressure and total temperature downstream of the rotor were each measured with a

pair of 5-element rakes placed 2.0 in. behind the rotor. These were similar to the upstream rakes, except that the pressure probes were of the directionally insensitive Kiel design. Radial traverses were made to measure total pressure and flow angle at locations 0.5 and 2.0 in. behind the rotor. Two- and three-hole prism-type yaw probes were used for measuring flow angle and flow angle plus total pressure. A row of static pressure taps of 0.025-in. diam were located in the outer casing beginning upstream, across, and downstream of the rotor. Additional static taps were placed at corresponding locations on the hub wall, up and downstream of the rotor.

The aerodynamic pressure data were measured with strain-gage transducers, and temperatures were measured with thermocouples. The outputs from these instruments are processed through an analog-to-digital converter and recording system. This system completed a scan of 100 channels in one minute.

SECTION III PROCEDURE

The compressor rotors were tested between 50 and 100 percent design speed in increments of 10-percent speed. Design corrected tip speed was 1600 ft/sec. Performance data were measured at each speed from choked flow (wide open throttle) to audible surge. Three complete data scans were recorded at each test point, and the average values were used in the data reduction process. The yaw probes were traversed once during each test point.

SECTION IV RESULTS AND DISCUSSION

4.1 GENERAL ROTOR PERFORMANCE

4.1.1 Rotor 1, Configuration 1

Complete experimental data for this configuration are presented as curves and tables in Appendix IV. Maximum design-speed pressure ratio was 2.34, at which point the adiabatic efficiency was 59 percent. Peak efficiency continuously increased as speed was reduced, reaching 76 percent at 50 percent speed. The relative inlet Mach number at design speed, and maximum pressure ratio, varied from 1.45 at the hub to about 1.56 at the tip.

Radial traverse data taken 0.5 in. downstream of the rotor show that flow separation occurred on the outer casing wall immediately downstream of the rotor at 90- and 100-percent speed. At 80-percent speed and below, this condition was not observed. From a comparison of data

over the speed range, it appears that relatively thick boundary layers develop in the blade passages as speed is increased and that much of this low-energy flow is centrifuged toward the tip as a secondary flow. This is probably a result of shock-induced suction surface separation leading to large cross flows in the separated region. The low-energy flow is unable to overcome the pressure gradient in the diffusion zone following the thick trailing edges at the higher speeds. This seriously distorts the rotor discharge profiles at intermediate speeds also.

The static pressure distributions along the annulus walls are tabulated in Appendix IV. At 100-percent speed, the compressor map showed that stall occurred before the bow shock was expelled from the flow passage between rotor blades, as evidenced by the vertical characteristic. This is confirmed by the casing static pressure distribution which shows a large passage entrance expansion before the first strong shock. At 90-percent and lower speeds, this entrance expansion is not evident at maximum back pressure. The annulus wall separation zone also produces a noticeable effect on the static pressure distributions. When separation occurs, the pressure gradient is sharply reduced.

The measured performance of this rotor is compared with some theoretical calculations in Ref. 3.

4.1.2 Rotor 1, Configuration 2

The experimental data for this configuration are also presented in Appendix IV. Maximum design-speed pressure ratio was 2.32, at which point the adiabatic efficiency was 57 percent. Peak efficiency continuously increased as speed was reduced, reaching 79 percent at 50 percent speed. The relative inlet Mach number distribution at design speed, and maximum pressure ratio, was the same as for Configuration 1.

The general remarks concerning the radial traverse data and static pressure distributions on the annulus walls are essentially the same for Configuration 2 as for Configuration 1. The difference in performance between these two configurations are discussed in Sect. 4.2.

4.2 COMPARISON BETWEEN ROTORS

The performance of the first and second configurations of Rotor 1 is compared over the entire speed range but in detail only at design speed. The compressor maps of the two configurations are superposed in Figs. 4 and 5 for 60-, 80-, and 100-percent design speed. At design speed, very little difference in performance is observed in total pressure ratio, isentropic efficiency, or mass flow. The effect of opening up the rotor flow passage, according to Ref. 3, was supposed to be an increase in rotor diffusion, thereby a decrease in dumping losses and an increase in pressure ratio and efficiency. The increased performance was expected only if boundary-layer blockage in the rotor did not increase a corresponding amount. From the experimental compressor

maps, it appears that blockage increased in nearly exact proportion to the increase in passage area because no improvement was observed. This is discussed in Sect. V.

At lower speeds, the second configuration choked at a higher value of mass flow than the first configuration. Since the effect of boundary-layer blockage and flow separation decrease with decreasing back pressure and rotor speed, the increase in flow with the second configuration is logical. As speed was reduced from 100 to 80 percent, the stalling value of total pressure ratio and of efficiency achieved with the second configuration dropped below those values achieved with the first. However, as speed decreased further to 60 percent and below, the stalling total pressure ratio of the second configuration recovered to that of the first and the peak efficiency exceeded that of the first. It appears that at supersonic and transonic speeds, the rotor boundary layers were not capable of sustaining the additional diffusion demanded by the greater blade-passage divergence of the second configuration. At subsonic speeds, the diffusion was evidently not excessive and the performance benefited because of the reduced velocity arriving at the abrupt trailing-edge diffusion zone. However, the range of flow between stall and choke was reduced for the second configuration at all speeds below design speed.

The annulus wall static pressure distribution measured at design speed and maximum back pressure is shown for each configuration, superposed in Fig. 6. The distribution has the same character for both configurations, although a slightly higher static pressure level is noted for Configuration 2. However, the higher static pressure rise experienced with the second configuration does not appear to be due to the higher over-all diffusion expected, since mass-averaged performance at this point was virtually unchanged. Rather, it seems to reflect a change in the radial distribution of the flow, which was less distorted with Configuration 2, having more diffusion near the tip and less diffusion near the hub. The dip in static pressure just downstream of the rotor is evident for both configurations. As mentioned in Ref. 3, this is characteristic of a local zone of boundary-layer separation on the casing wall.

Radial distributions of various parameters, measured 2 in. downstream of the rotor at design speed, and maximum back pressure, are superposed for the two configurations in Figs. 7 through 12. The differences in performance between the two configurations are slight. However, the uniformity of all plotted quantities was somewhat better with Configuration 2. A drastic fall-off in specific mass flow is evident for both configurations in the outer 50 percent of the annulus. This is probably attributable to the casing boundary-layer separation bubble which is located between the 2-in. downstream measuring station and the rotor. The corresponding absolute flow angle also increases sharply in this same zone.

SECTION V CONCLUSIONS

The major conclusion to be drawn from these two experiments is that the configurations tested demanded too much diffusion for either the rotor or the downstream diffusion zone to handle efficiently. Although the blunt trailing edges limited diffusion within the blade row, the lack of any annulus convergence caused a very rapid diffusion and subsequent boundary-layer separation downstream.

A second conclusion may be drawn from the observation that the modification of Configuration 1 to produce Configuration 2 (namely, increasing rotor flow passage divergence) does not lead to an increase in performance. The mathematical model presented in Ref. 3 showed that, if boundary-layer blockage within the blade row did not increase, more diffusion should take place within the blade row. Thus, the losses leaving the blade row would be reduced, causing an overall increase in performance. Since this did not occur, and since stall occurred at nearly the same pressure ratios as before, it might be concluded that the blockage term employed in the theory does not really represent boundary-layer blockage but indicates the size of the separation zone between blades. The flow is expected to separate on the suction surface of each blade, at or near design speed, where the bow shock of each adjacent blade impinges. If little or no reattachment takes place, opening up the passage may produce virtually no change in the fluid mainstream and only move the free surface of the fluid a corresponding amount further away from the suction surface of each blade.

At subsonic speeds, 60-percent design for example, efficiency was increased at the expense of flow range, and stalling pressure ratio remained about the same. It may be concluded for this condition that separation was no longer a factor before the stall point was reached and that the increased divergence of the passage did produce increased rotor diffusion, leading to equivalent pressure ratios at higher mass flows.

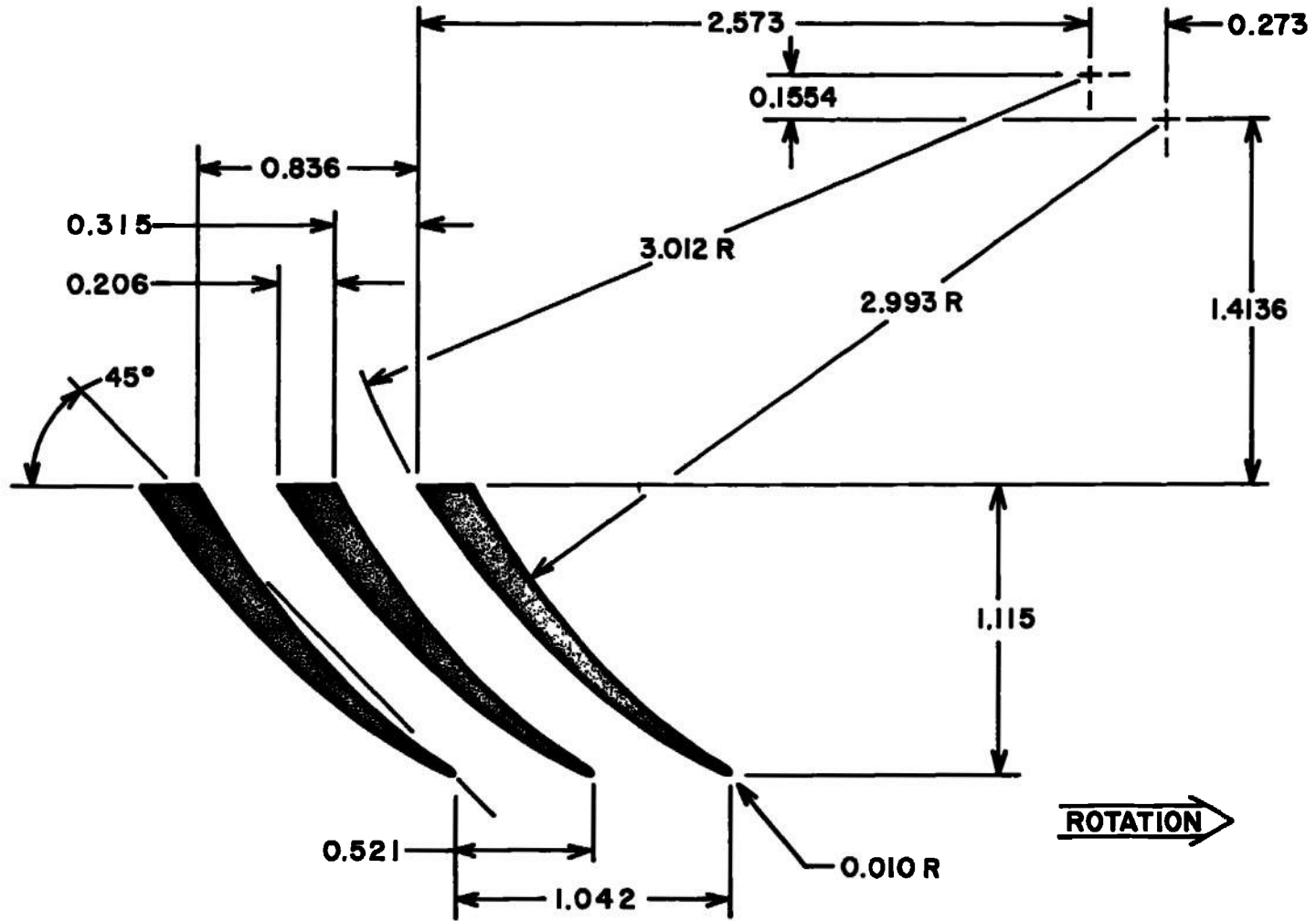
REFERENCES

1. Johnson, E. G., von Ohain, H., Lawson, M. D., and Cramer, K. R. "A Blunt-Trailing-Edge Supersonic Compressor Blading." WADC TN 59-269, 1959.
2. Chauvin, J. "The Concept of Blunt-Trailing-Edge Blading for Use in Supersonic Compressors." Paper DK 533-697-242-011.5, Jahrbuch 1962 der WFLR, Vieweg and Sohn, Braunschweig, Germany, 1963.
3. Wennerstrom, A. J. and Olympios, S. "A Theoretical Analysis of the Blunt-Trailing-Edge Supersonic Compressor and Comparison with Experiment." ARL 66-0236, 1966.

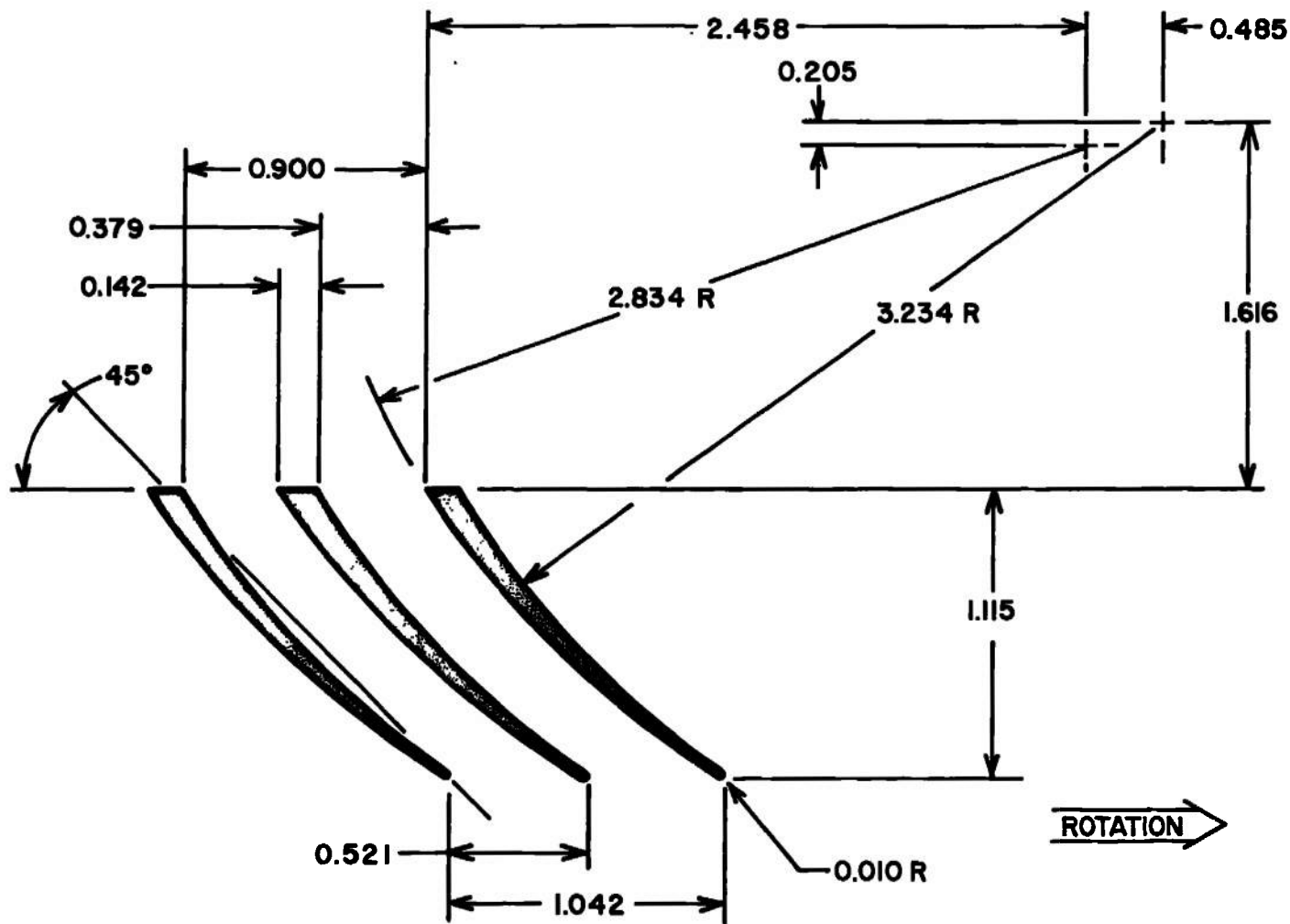
4. Chauvin, J. "Research on the Concept of Blunt-Trailing-Edge Blades," von Karman Institute for Fluid Dynamics, Rhode St.-Genese, Belgium, 1965.
5. Carman, C. T. "Development of the Supersonic Compressor Test Facilities at the Arnold Engineering Development Center." AEDC-TR-65-169 (AD 471021), 1965.

APPENDIXES

- I. ILLUSTRATIONS**
- II. METHODS OF CALCULATION**
- III. MEASUREMENT UNCERTAINTY**
- IV. DATA SUMMARY FOR CONFIGURATIONS 1 AND 2**



a. Blunt-Trailing-Edge Blade Configuration 1
 Fig. 1 Blade Geometry of Mean Radius Profile



b. Blunt-Trailing-Edge Blade Configuration 2
Fig. 1 Concluded

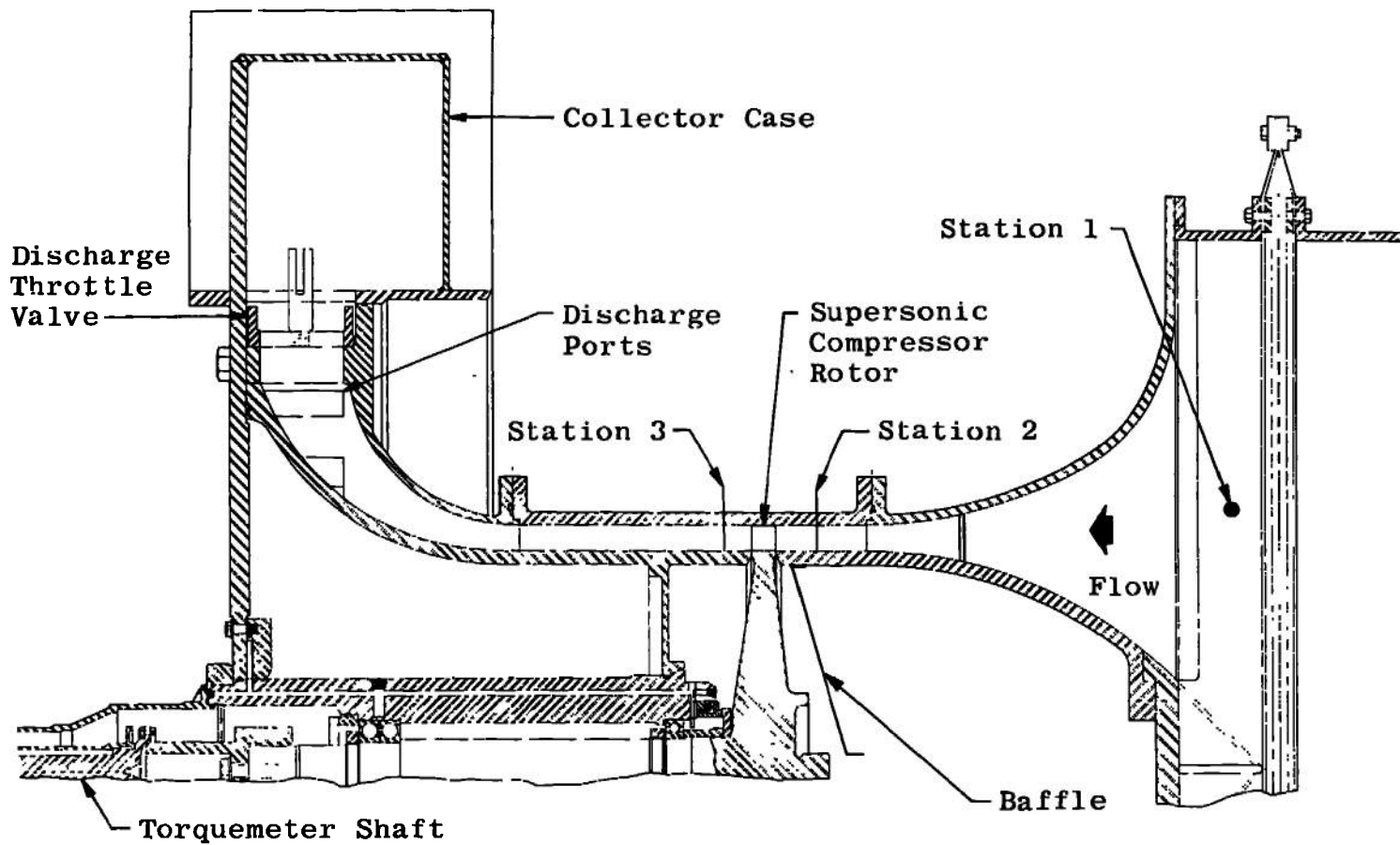
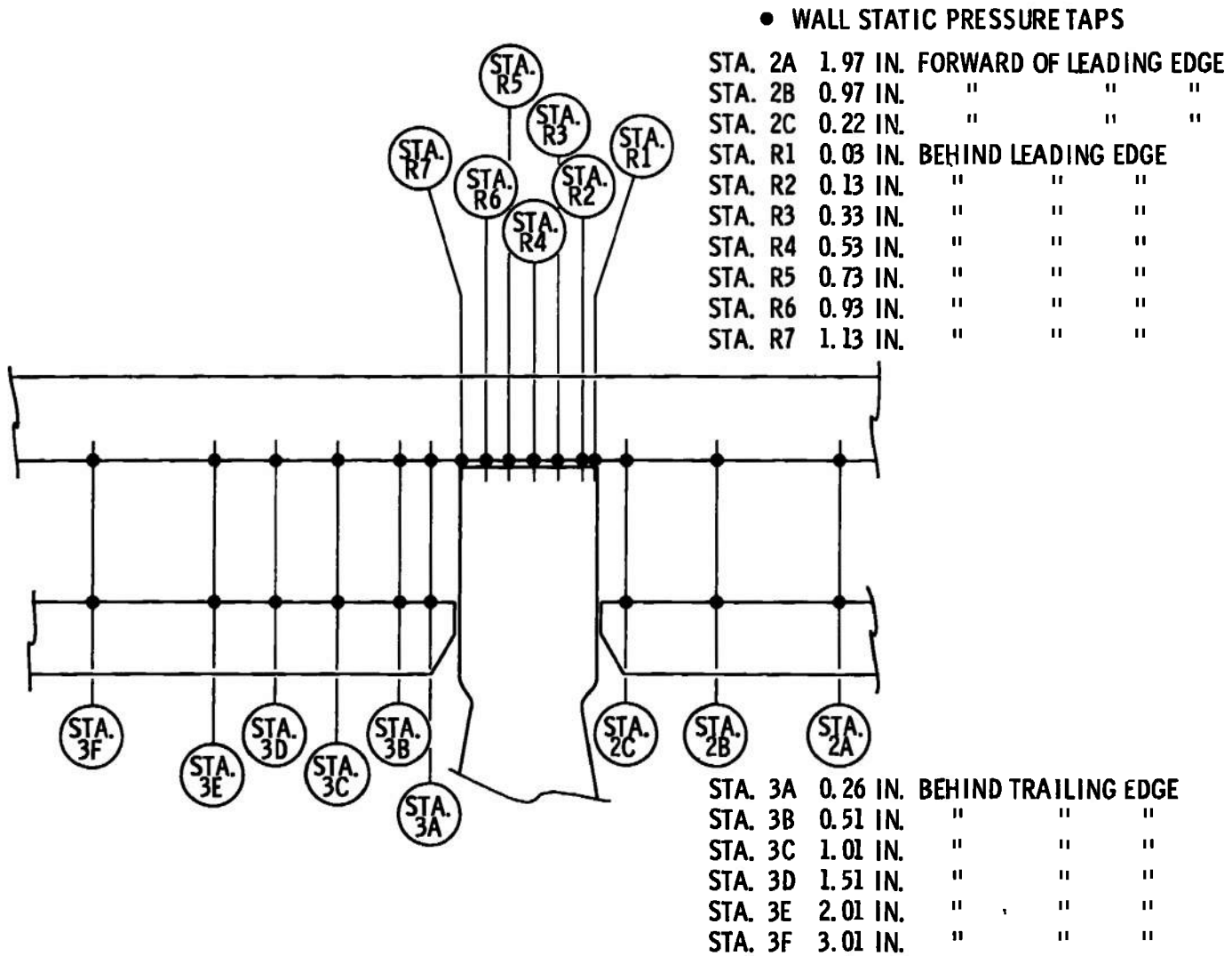
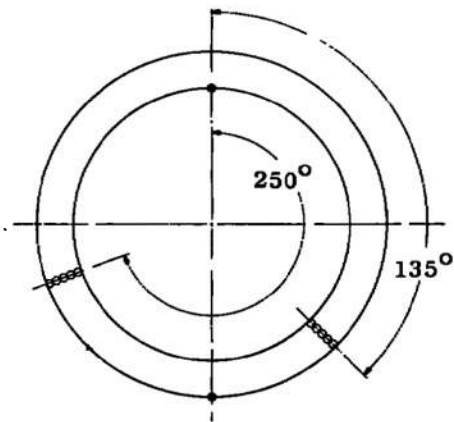


Fig. 2 Cross-Sectional View of Experimental Compressor

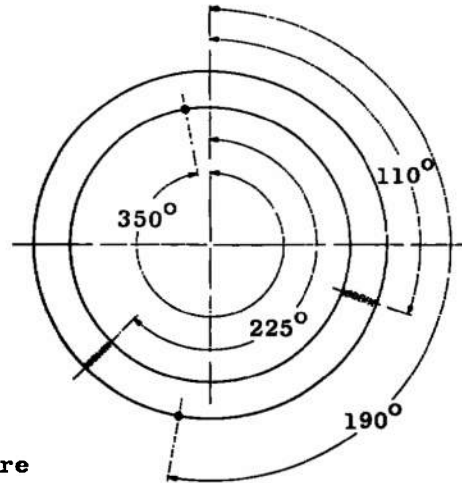


a. Station Locations

Fig. 3 Details of Instrumentation Stations

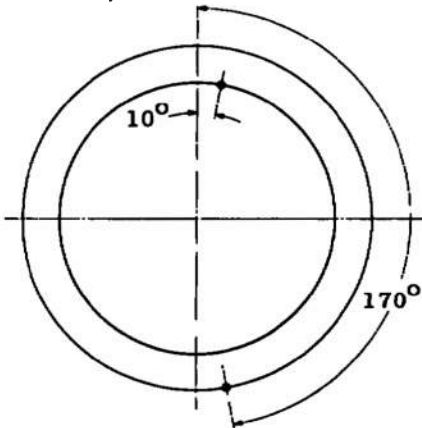


b. Station 2A

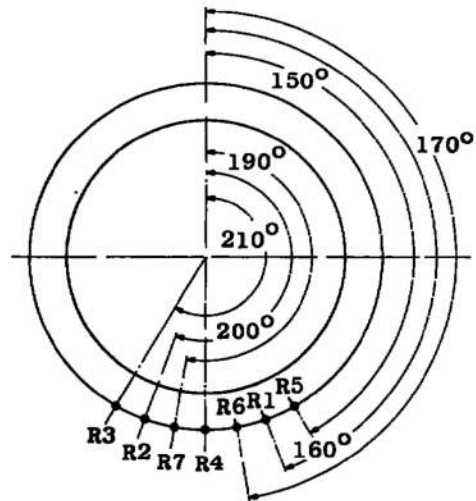


c. Station 2B

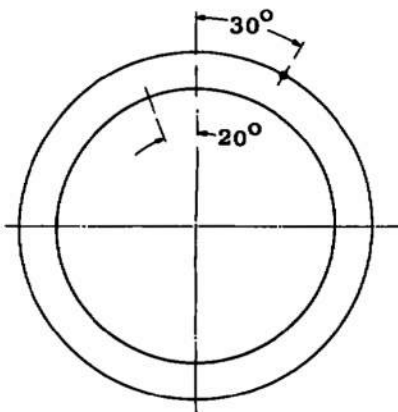
- o Total Pressure
- Static Pressure
- x Total Temperature
- ↓ Traverse
- ↷ Yaw Angle



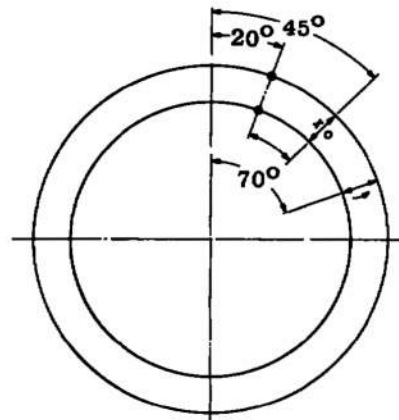
d. Station 2C



e. Station R1 - R7

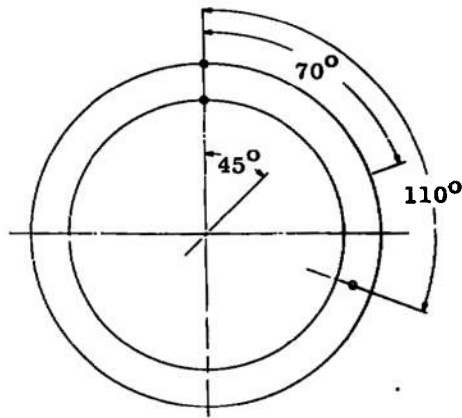


f. Station 3A

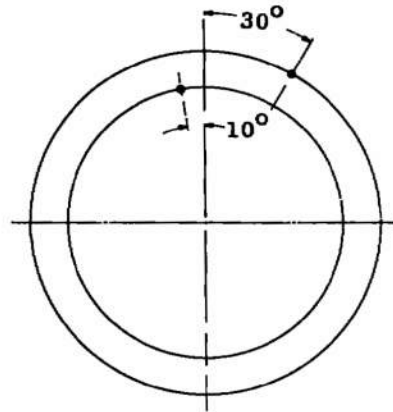


g. Station 3B

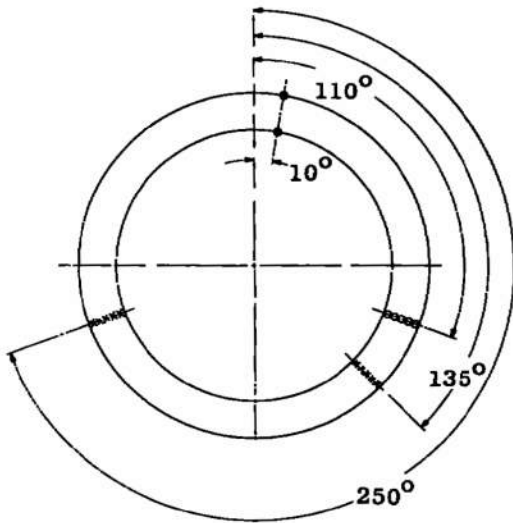
Fig. 3 Continued



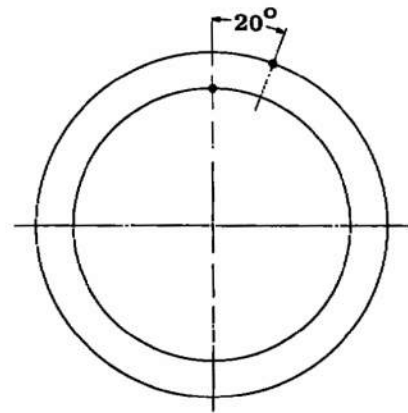
h. Station 3C



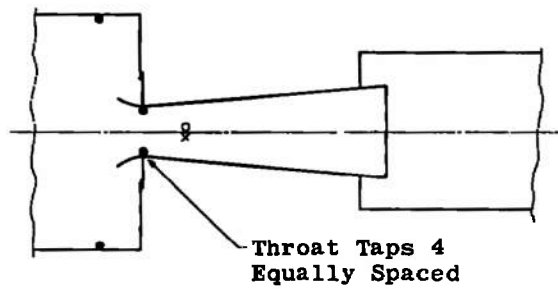
i. Station 3D



j. Station 3E



k. Station 3F



l. Venturi Instrumentation

Fig. 3 Concluded

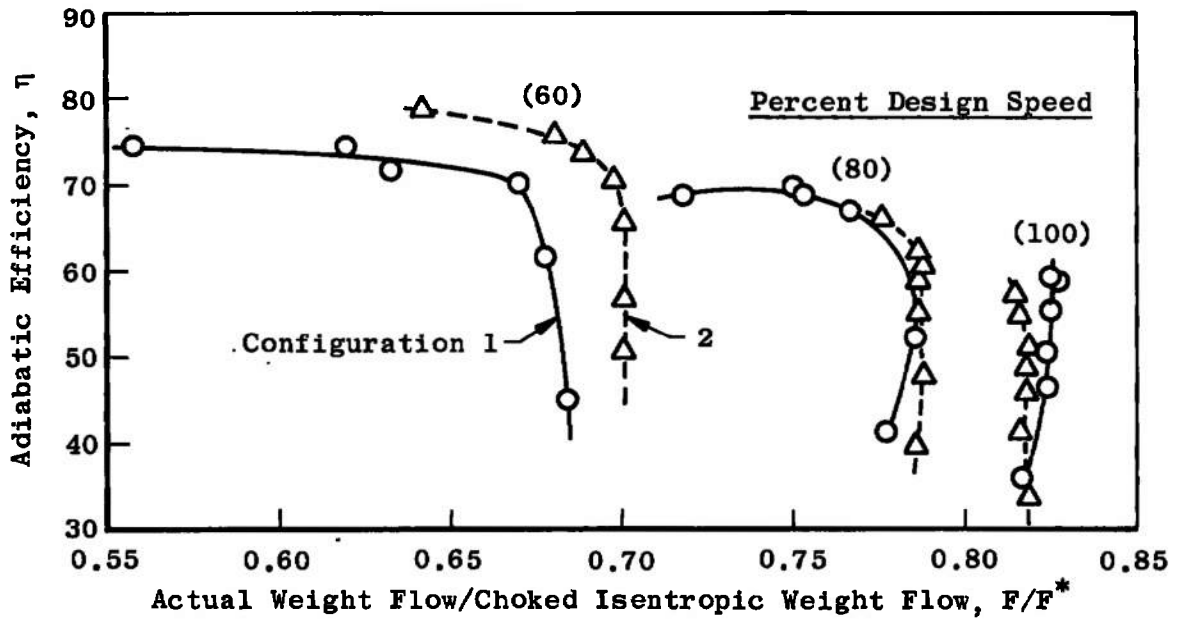


Fig. 4 Rotor Isentropic Efficiency

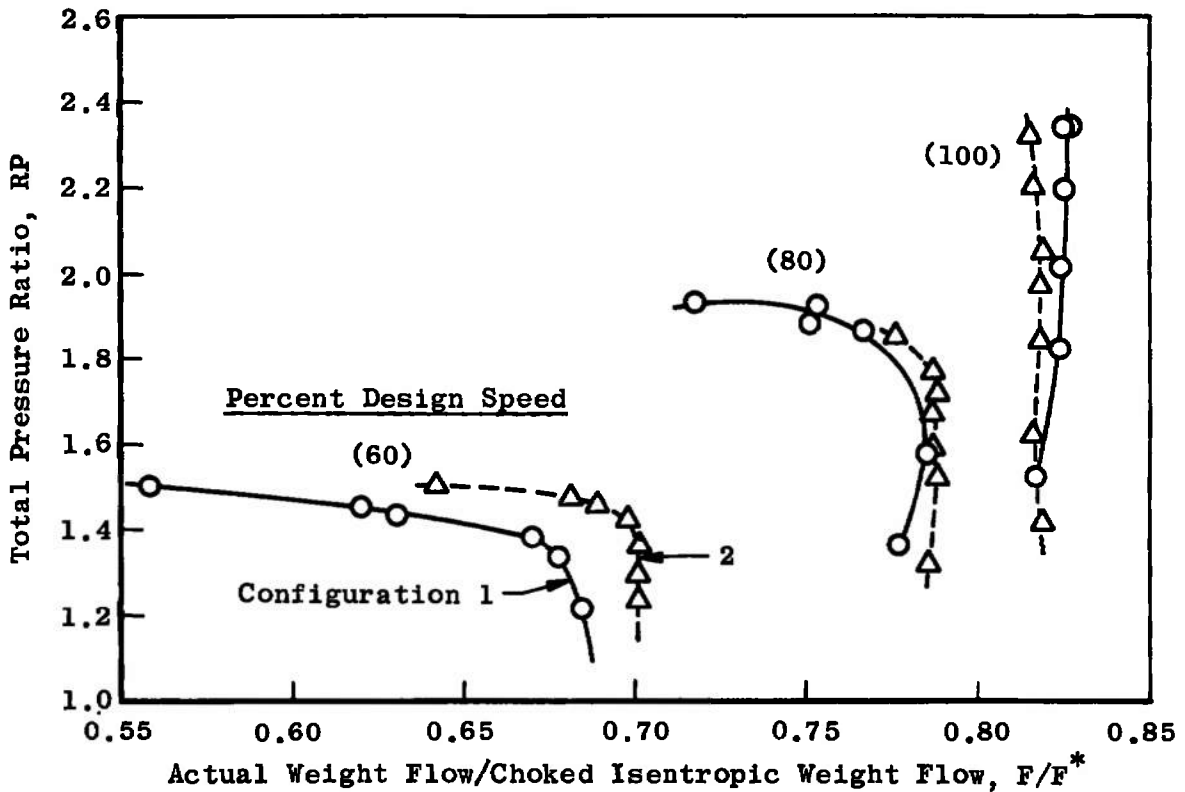


Fig. 5 Rotor Total Pressure Ratio

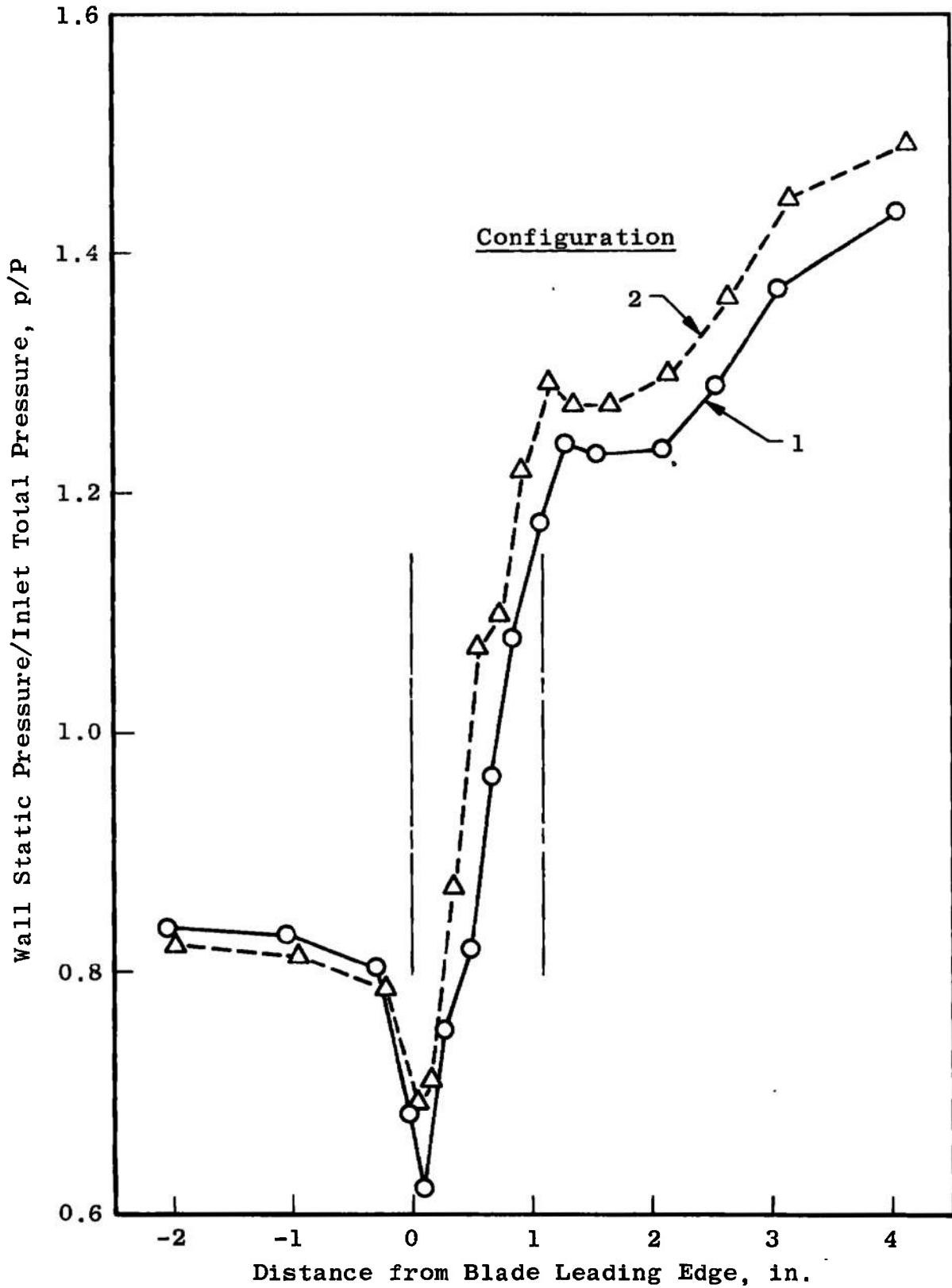


Fig. 6 Casing Static Pressure Distribution at Design Speed and Maximum Back Pressure

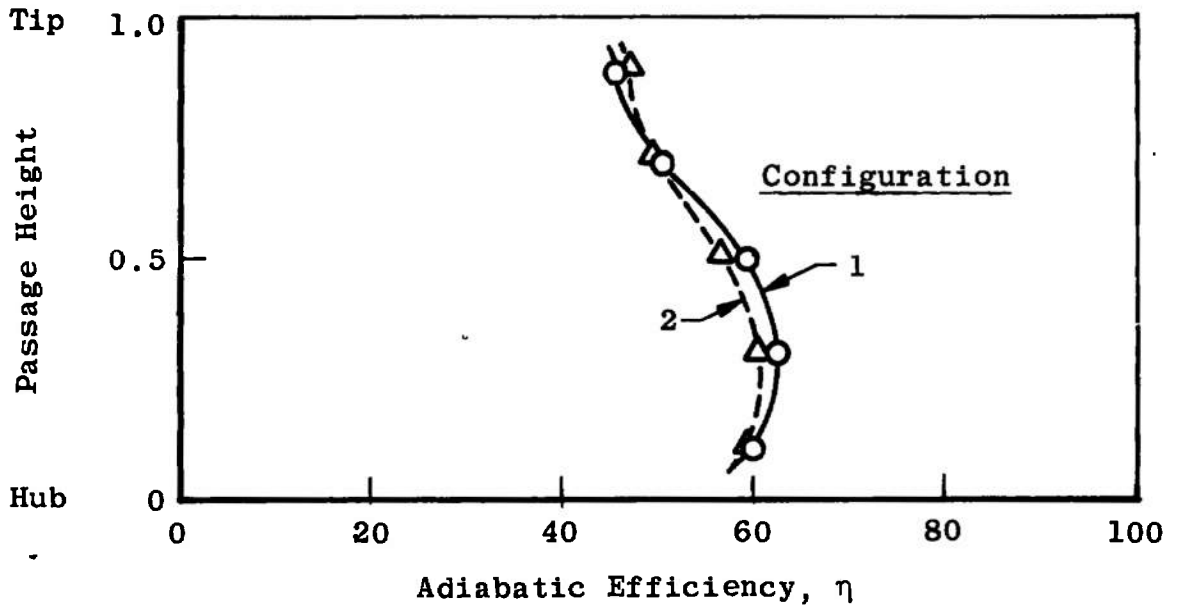


Fig. 7 Efficiency Distribution at Design Speed and Maximum Back Pressure

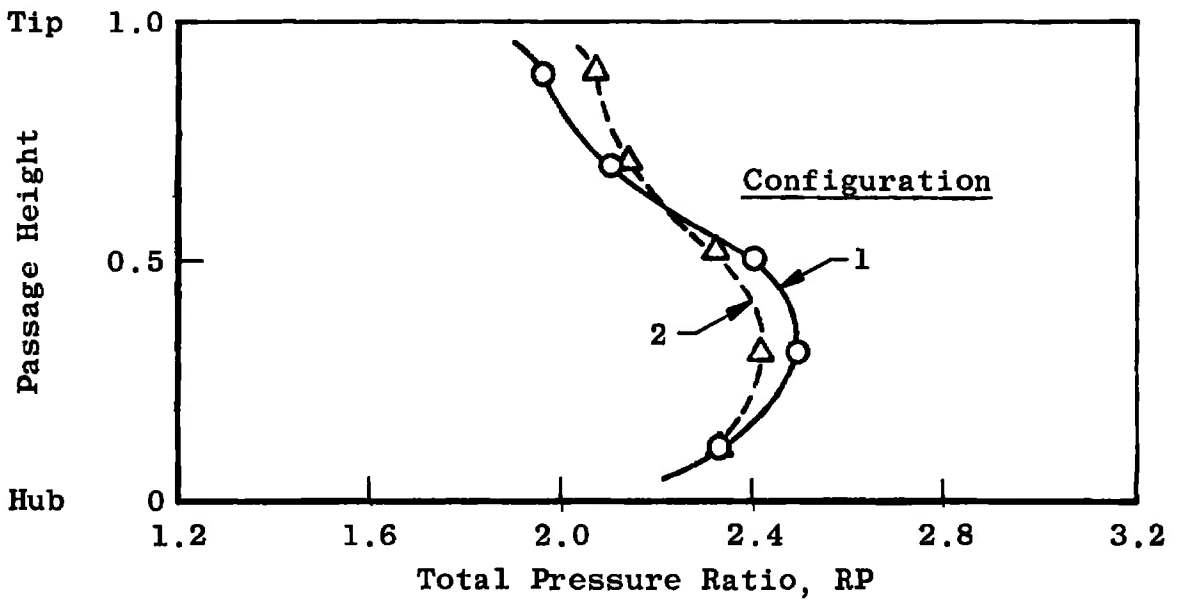


Fig. 8 Total Pressure Distribution at Design Speed and Maximum Back Pressure

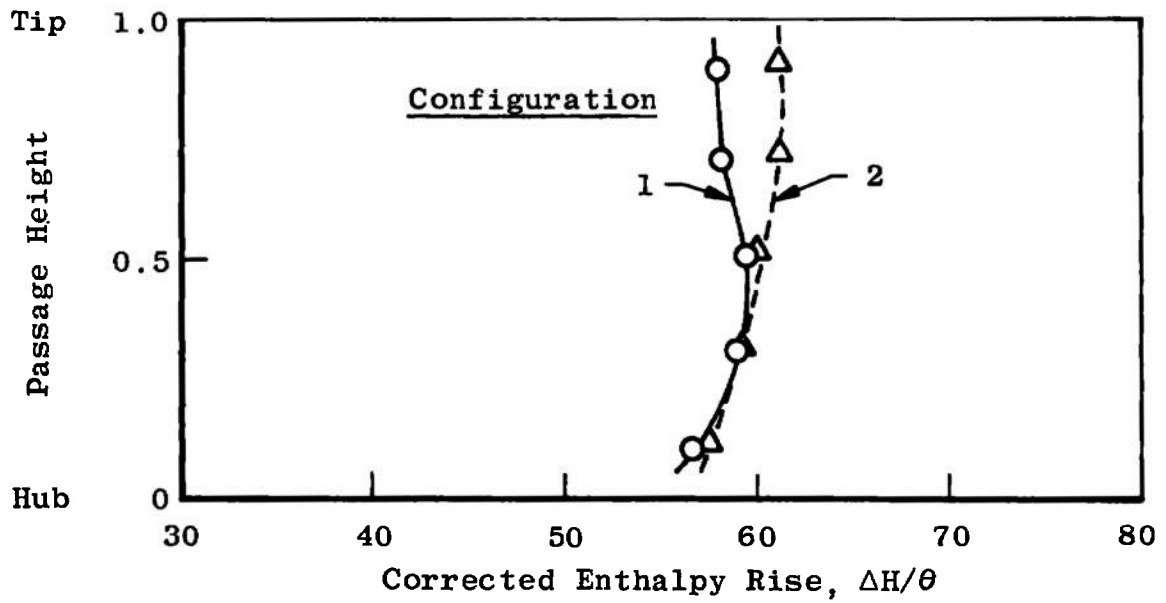


Fig. 9 Corrected Enthalpy Rise at Design Speed and Maximum Back Pressure

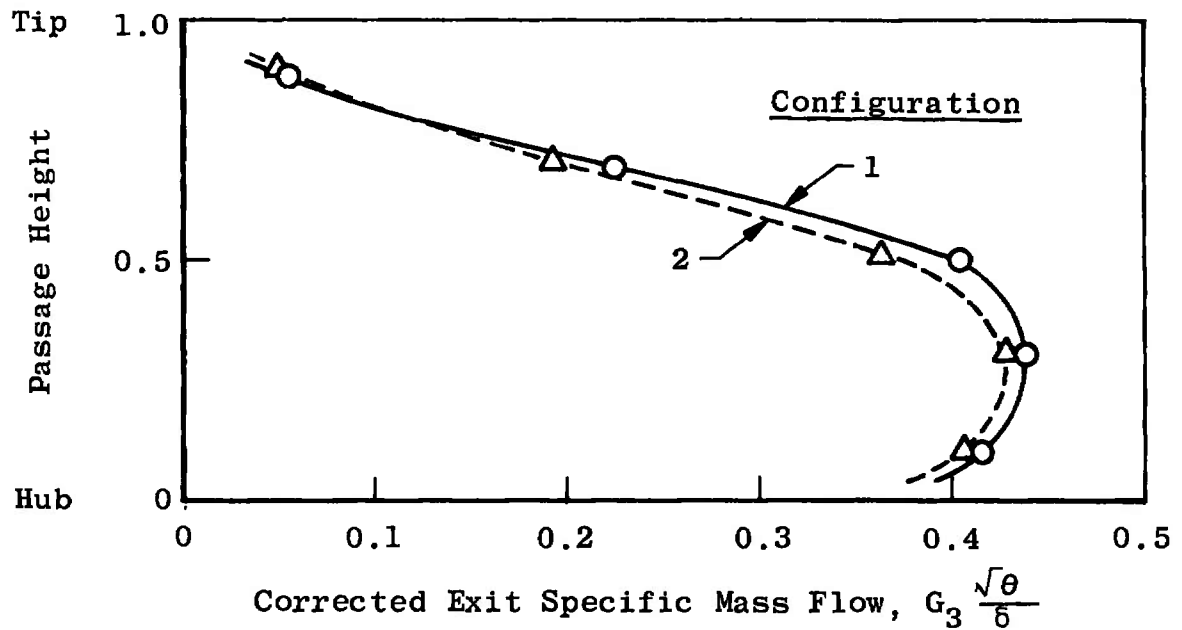


Fig. 10 Specific Mass Flow Distribution at Design Speed and Maximum Back Pressure

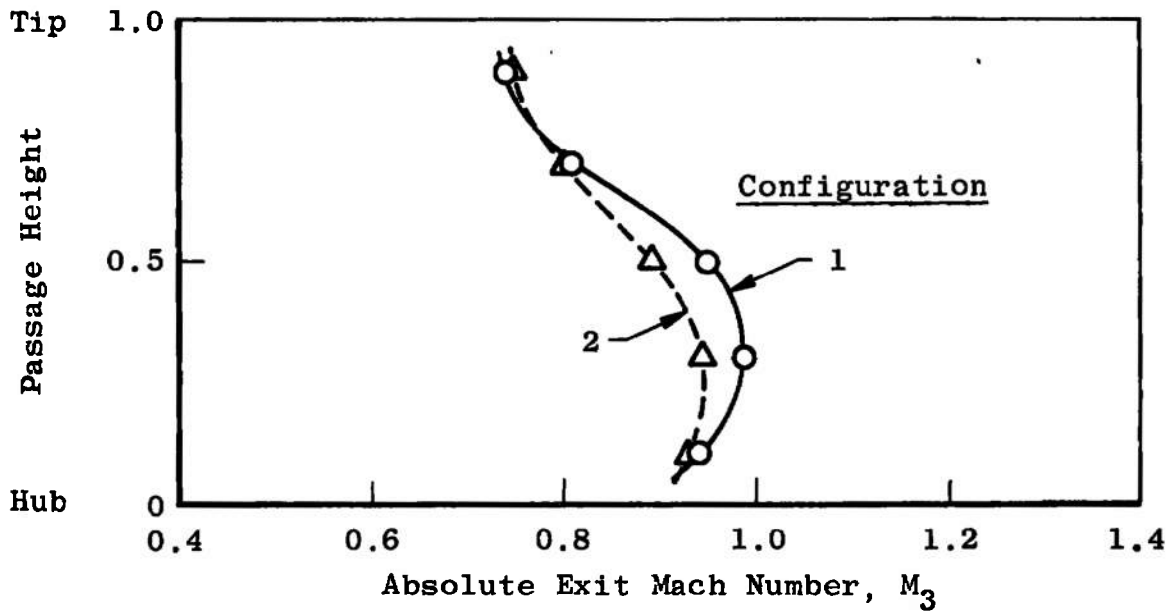


Fig. 11 Absolute Exit Mach Number Distribution at Design Speed and Maximum Back Pressure

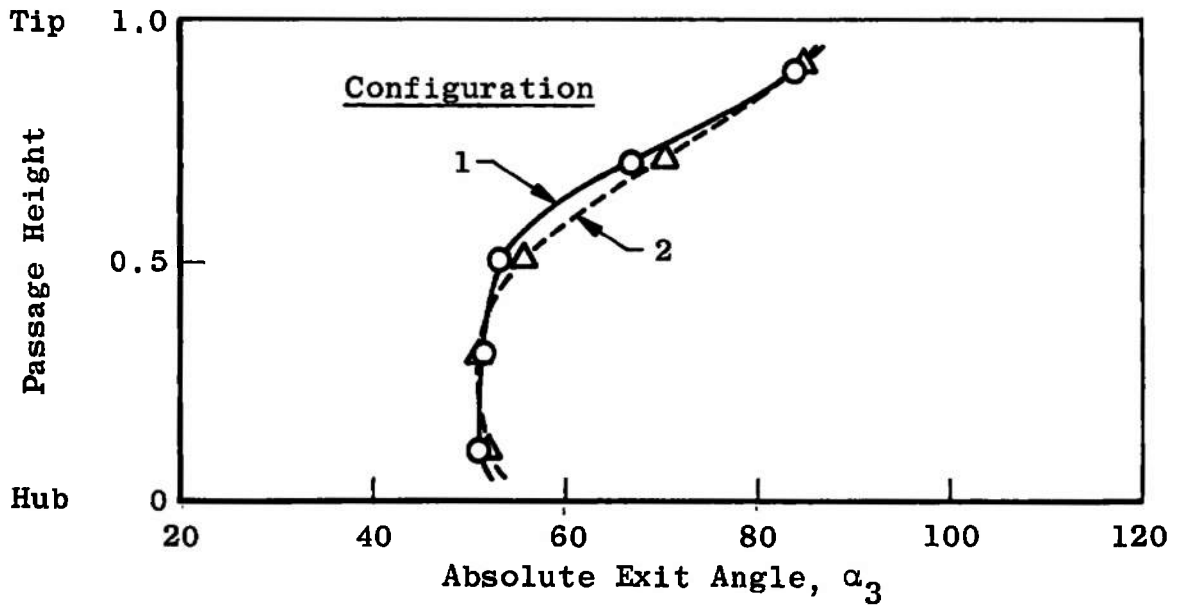


Fig. 12 Absolute Exit Flow Angle Distribution at Design Speed and Maximum Back Pressure

APPENDIX II METHODS OF CALCULATION

General methods and equations employed to compute the parameters presented are given herein. Test data were processed to the final parameters with an IBM 360/50 digital computer.

TEMPERATURE

Discharge total temperatures were corrected by applying a recovery factor of 0.96 to the indicated temperature measurements in the calculation:

$$T_3 = \frac{T_i(\gamma M^2 - M^2 + 2)}{RF(\gamma M^2 - M^2) + 2}$$

Static temperatures were calculated from the measured stagnation temperatures and pressures by using perfect gas, isentropic relations:

$$t = T \left(\frac{P}{P}\right)^{\frac{\gamma-1}{\gamma}}$$

The static pressure values across the passage were assumed as a linear variation from the measured static pressures at the walls.

SPECIFIC HEAT

The specific heat at constant pressure was computed from the empirical equation:

$$C_p = 0.2318 + 0.104 \times 10^{-4} T + 0.7166 \times 10^{-8} T^2$$

The ratio of specific heats was assumed to be 1.4 at the venturi and inlet stations. At all other stations the ratio of specific heats was calculated from the expression

$$\gamma = \frac{C_p}{C_p - \frac{R}{J}}$$

When applicable, arithmetic averages of the specific heat ratios were used.

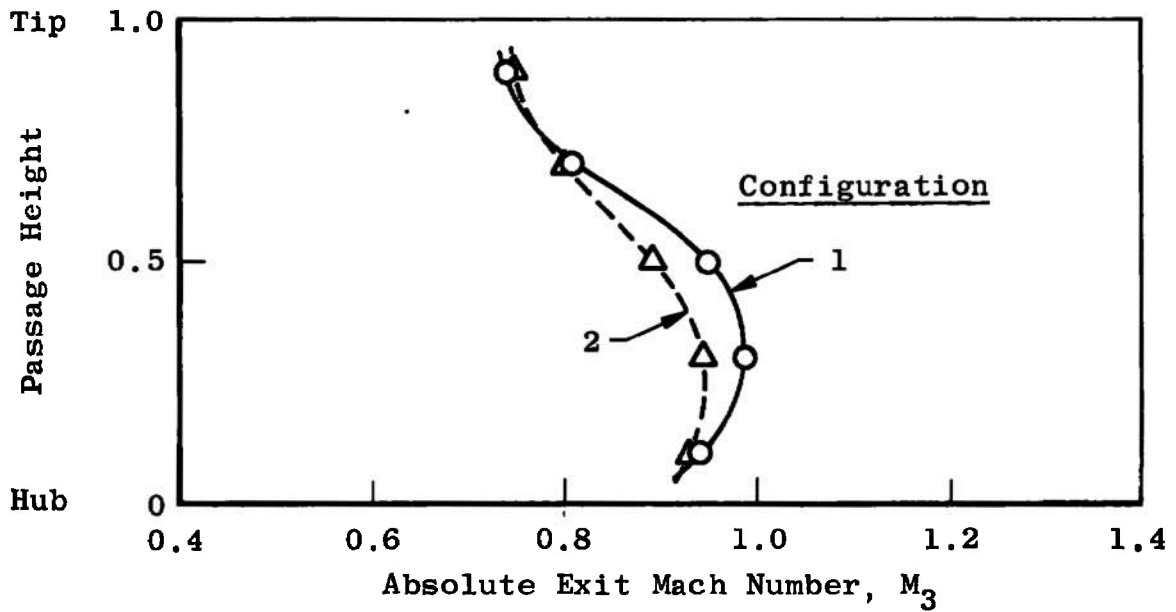


Fig. 11 Absolute Exit Mach Number Distribution at Design Speed and Maximum Back Pressure

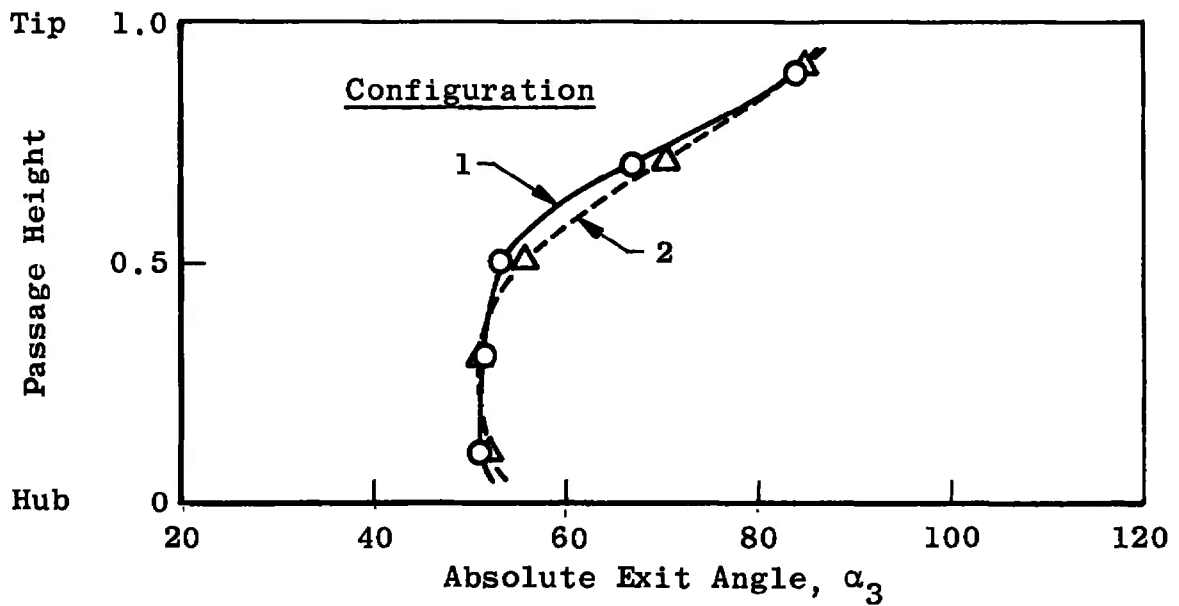


Fig. 12 Absolute Exit Flow Angle Distribution at Design Speed and Maximum Back Pressure

APPENDIX II METHODS OF CALCULATION

General methods and equations employed to compute the parameters presented are given herein. Test data were processed to the final parameters with an IBM 360/50 digital computer.

TEMPERATURE

Discharge total temperatures were corrected by applying a recovery factor of 0.96 to the indicated temperature measurements in the calculation:

$$T_3 = \frac{T_i(\gamma M^2 - M^2 + 2)}{RF(\gamma M^2 - M^2) + 2}$$

Static temperatures were calculated from the measured stagnation temperatures and pressures by using perfect gas, isentropic relations:

$$t = T\left(\frac{P}{P}\right)^{\frac{\gamma-1}{\gamma}}$$

The static pressure values across the passage were assumed as a linear variation from the measured static pressures at the walls.

SPECIFIC HEAT

The specific heat at constant pressure was computed from the empirical equation:

$$C_p = 0.2318 + 0.104 \times 10^{-4} T + 0.7166 \times 10^{-8} T^2$$

The ratio of specific heats was assumed to be 1.4 at the venturi and inlet stations. At all other stations the ratio of specific heats was calculated from the expression

$$\gamma = \frac{C_p}{C_p - \frac{R}{J}}$$

When applicable, arithmetic averages of the specific heat ratios were used.

AIRFLOW

Airflow was calculated at the venturi from the following equation using a flow coefficient (C_f) of 0.99:

$$F = C_f A P \left[\frac{2\gamma g}{RT(\gamma - 1)} \left(\left[\frac{P}{P} \right]^{\frac{2}{\gamma}} - \left[\frac{P}{P} \right]^{\frac{\gamma + 1}{\gamma}} \right) \right]^{1/2}$$

ABSOLUTE MACH NUMBER

Mach number was obtained from the compressible flow equation:

$$M = \left(\frac{2}{\gamma - 1} \right)^{1/2} \left[\left(\frac{P}{P} \right)^{\frac{\gamma - 1}{\gamma}} - 1 \right]^{1/2}$$

ADIABATIC EFFICIENCY

The adiabatic efficiency was computed from the following expressions:

$$\eta = \frac{\Delta H_{\text{ideal}}}{\Delta H_{\text{actual}}}$$

where

$$\Delta H = \int_{T_2}^{T_3} C_p dT$$

$$\text{Ideal } T_3 = T_2 \left(\frac{P_3}{P_2} \right)^{\frac{\gamma - 1}{\gamma}}$$

$$\text{Actual } T_3 = T_3 \text{ measured}$$

VELOCITY

Velocity was determined from the expression:

$$C = \left(\frac{2\gamma Rgt}{\gamma - 1} \right)^{1/2} \left[1 - \left(\frac{P}{P} \right)^{\frac{\gamma - 1}{\gamma}} \right]^{1/2}$$

RELATIVE FLOW ANGLE

Relative flow angle to the blade was obtained by

$$\beta = \arctan \frac{U - C \sin \alpha}{C \cos \alpha}$$

where

$$U = \frac{2\pi}{60} r N$$

RELATIVE MACH NUMBER

Relative Mach number to the blade was determined by

$$M_w = \frac{W}{C} \frac{1}{M}$$

where

$$W = \frac{U - C \sin \alpha}{\sin \beta}$$

MASS-WEIGHTING FACTOR

Specific mass flow is used as a weighting factor in the summation of various parameters computed from data measured in the five equal areas across the annulus passage and is calculated by

$$G = pM \left(\frac{\rho \gamma}{RT} \right)^{1/2} \cos \alpha$$

APPENDIX III MEASUREMENT UNCERTAINTY

Physical measurements involve two basic classes of error - precision or repeatability error and accuracy error. Precision error is present when successive measurements of an unchanged quantity yield different numerical results. Accuracy error is present when the numerical average of successive readings deviates from the known correct reading and continues to do so no matter how many successive readings are taken.

Accuracy error is eliminated by calibration. The total pressure probes have been calibrated aerodynamically. Total temperature probes have been calibrated in an oil bath (see references).

Without a great many replications of readings with the entire measurement system, precision error can only be estimated from manufacturers' specifications for each component of the system. Tables III-I and III-II show the estimated precision for the instrumentation of, respectively, configurations 1 and 2. In these tables the system sensor implies the transducer in the case of pressure measurements and the thermocouple junction for the temperature measurements. Transmission error for temperature measurements depends on the wire used. Reference errors may involve the accuracy in reading atmospheric pressure or some base reference. Read-out error includes both interpretation and digitizing error. The total precision is the arithmetic sum of these values. If calibration has been used to eliminate accuracy error, these figures represent the total uncertainty of a single measurement.

The final column of Tables III-I and III-II presents the number of times a single point is replicated. Traverse measurements are manually read while rake data are electronically recorded. During one traverse there is time to make three complete scans of rake data. Since error in an average is inversely proportional to the square of the number of readings making up the average,¹ it is felt that the rake measurements probably represent the more accurate values.

The precision index W_R of a general function R where

$$R = f(x_1, x_2, \dots, x_n)$$

may be calculated by

$$W_R = \left[\sum_{i=1}^n \left(\frac{\partial R}{\partial x_i} \right)^2 W_i^2 \right]^{1/2}$$

¹Hilbert, Shenck, Jr. Theories of Engineering Experimentation. McGraw-Hill Book Company, New York, N. Y., 1961.

where W_i is the precision of the independent variables. Using this relation and the estimated precision of Tables III-I and III-II and assuming constant specific heat at constant pressure, the estimated precision in total pressure ratio, RP, adiabatic efficiency, η , inlet absolute Mach number, M_2 , and outlet absolute Mach number, M_3 , is calculated at the extremes of operating conditions. Inlet stagnation conditions are assumed standard.

The following table summarizes the results of the computation where the precisions indicated represent approximately twice the standard deviation.

CONFIGURATION 1

| | W_{RP} | W_N | W_{M_2} | W_{M_3} |
|----------|-------------|-------------|-------------|-------------|
| 1.0N Max | ± 0.021 | ± 0.017 | ± 0.004 | ± 0.001 |
| 0.5N Min | ± 0.013 | ± 0.088 | ± 0.005 | ± 0.004 |

CONFIGURATION 2

| | W_{RP} | W_N | W_{M_2} | W_{M_2} |
|----------|-------------|-------------|-------------|-------------|
| 1.0N Max | ± 0.014 | ± 0.015 | ± 0.002 | ± 0.001 |
| 0.5N Min | ± 0.011 | ± 0.072 | ± 0.002 | ± 0.004 |

The apparent large uncertainty in efficiency at low-speed operation is not born out in repeated measurements near this condition. Precision in efficiency based on seven data points at 0.6N minimum pressure ratio is computed to be approximately ± 0.020 .

Mass flow is measured by a venturi flowmeter with manometer board pressure measurements photographically recorded and temperature measurements recorded electronically. The precision of the mass flow measurements at 1.0N maximum pressure ratio is computed to be approximately $\pm 0.415 \text{ lb}_m/\text{sec}$. This value includes allowance for error in readings of atmospheric pressure and fluid column heights; fluid density change caused by variation in ambient temperature and manometer board temperature gradients; sensor, transmission, reference and read-out errors in temperature; round-off errors in millivolt to Fahrenheit degree conversion; venturi throat area measurement precision; and the flow coefficient.

Rpm is measured by a frequency counter for the output of an electromagnetic pickup. The accuracy is ± 1 count digitizing error, ± 0.04 percent of the reading caused by scale conversion, ± 10 counts error in reading during operation. At maximum rpm this amounts to ± 0.1 percent error.

**TABLE III-I
CONFIGURATION 1**

| <u>PARAMETER</u> | <u>SENSOR PRECISION</u> | <u>TRANSMISSION PRECISION</u> | <u>REFERENCE PRECISION</u> | <u>READ-OUT PRECISION</u> | <u>TOTAL PRECISION</u> | <u>REPETITION</u> |
|-------------------------------|-----------------------------|-----------------------------------|--------------------------------|-------------------------------|----------------------------|-------------------|
| <u>Total Pressure</u> | | | | | | |
| Inlet Rake | ±0.100 psi | | ±0.005 psi | ±0.015 psi | ±0.120 psi | 6 |
| Outlet Rake | ±0.125 psi | | | ±0.015 psi | ±0.140 psi | 3 |
| Outlet Traverse | ±0.125 psi | | | ±0.125 psi | ±0.250 psi | |
| <u>Static Pressure</u> | | | | | | |
| Inlet Wall 2A, 2B, 2C | ±0.100 psi | | ±0.005 psi | ±0.015 psi | ±0.120 psi | 3 |
| Wheel Wall TR1, 2, 3, 4 | ±0.100 psi | | ±0.005 psi | ±0.015 psi | ±0.120 psi | 3 |
| TR5, 6, 7 | ±0.500 psi | | ±0.005 psi | ±0.015 psi | ±0.520 psi | 3 |
| Outlet Wall 3A, 3B, 3E, 3F | ±0.125 psi | | | ±0.015 psi | ±0.140 psi | 3 |
| 3C, 3D | ±0.500 psi | | ±0.005 psi | ±0.015 psi | ±0.520 psi | 3 |
| <u>Total Temperature</u> | | | | | | |
| Inlet Rake | ±1°R | ±2.0°R | ±0.200°R | ±0.006MV(0.324°R) | ±3.524°R | 6 |
| Outlet Rake | ±1°R | ±2.0°R | ±0.200°R | ±0.006MV(0.324°R) | ±3.524°R | 6 |
| Outlet Traverse | ±1°R | ±2.0°R | ±0.875°R | ±1.0°R | ±4.875°R | 1 |
| <u>Absolute Flow Angle</u> | ±0.25 deg | | ±0.50 deg | ±0.50 deg | ±1.25 deg | 1 |

27

TABLE III-II
CONFIGURATION 2

| <u>PARAMETER</u> | <u>SENSOR PRECISION</u> | <u>TRANSMISSION PRECISION</u> | <u>REFERENCE PRECISION</u> | <u>READ-OUT PRECISION</u> | <u>TOTAL PRECISION</u> | <u>REPETITION</u> |
|-------------------------------|-----------------------------|-----------------------------------|--------------------------------|-------------------------------|----------------------------|-------------------|
| <u>Total Pressure</u> | | | | | | |
| Inlet Rake | ±0.050 psi | | | ±0.015 psi | ±0.065 psi | 6 |
| Outlet Rake | ±0.125 psi | | | ±0.015 psi | ±0.140 psi | 3 |
| Outlet Traverse | ±0.125 psi | | | ±0.125 psi | ±0.250 psi | 1 |
| <u>Static Pressure</u> | | | | | | |
| Inlet Wall 2A, 2B, 2C | ±0.050 psi | | | ±0.015 psi | ±0.065 psi | 3 |
| Wheel Wall TR1, 2, 3 | ±0.050 psi | | | ±0.015 psi | ±0.065 psi | 3 |
| TR4 | ±0.075 psi | | | ±0.015 psi | ±0.090 psi | 3 |
| TR5, 6, 7 | ±0.500 psi | | ±0.005 psi | ±0.015 psi | ±0.520 psi | 3 |
| Outlet Wall 3A, 3B, 3E, 3F | ±0.125 psi | | | ±0.015 psi | ±0.140 psi | 3 |
| 3C, 3D | ±0.500 psi | | ±0.005 psi | ±0.015 psi | ±0.520 psi | 3 |
| <u>Total Temperature</u> | | | | | | |
| Inlet Rake | ±1°R | ±2.0°R | ±0.200°R | ±0.006MV(0.324°R) | ±3.524°R | 6 |
| Outlet Rake | ±1°R | ±2.0°R | ±0.200°R | ±0.006MV(0.324°R) | ±3.524°R | 6 |
| Outlet Traverse | ±1°R | ±2.0°R | ±0.875°R | ±1.0°R | ±4.875°R | 1 |
| <u>Absolute Flow Angle</u> | ±0.25 deg | | ±0.50 deg | ±0.50 deg | ±1.25 deg | 1 |

**APPENDIX IV
DATA SUMMARY FOR CONFIGURATIONS 1 AND 2**

ILLUSTRATIONS

Fig. IV-1 Configuration 1

- a. Compressor Performance Characteristics Based on Equivalent Weight Flow
- b. Compressor Performance Characteristics Based on Weight Flow Ratio
- c. Inlet Parameters
- d. Exit Parameters
- e. Adiabatic Efficiency and Pressure Ratio
- f. Exit Specific Mass Flow and Enthalpy Rise

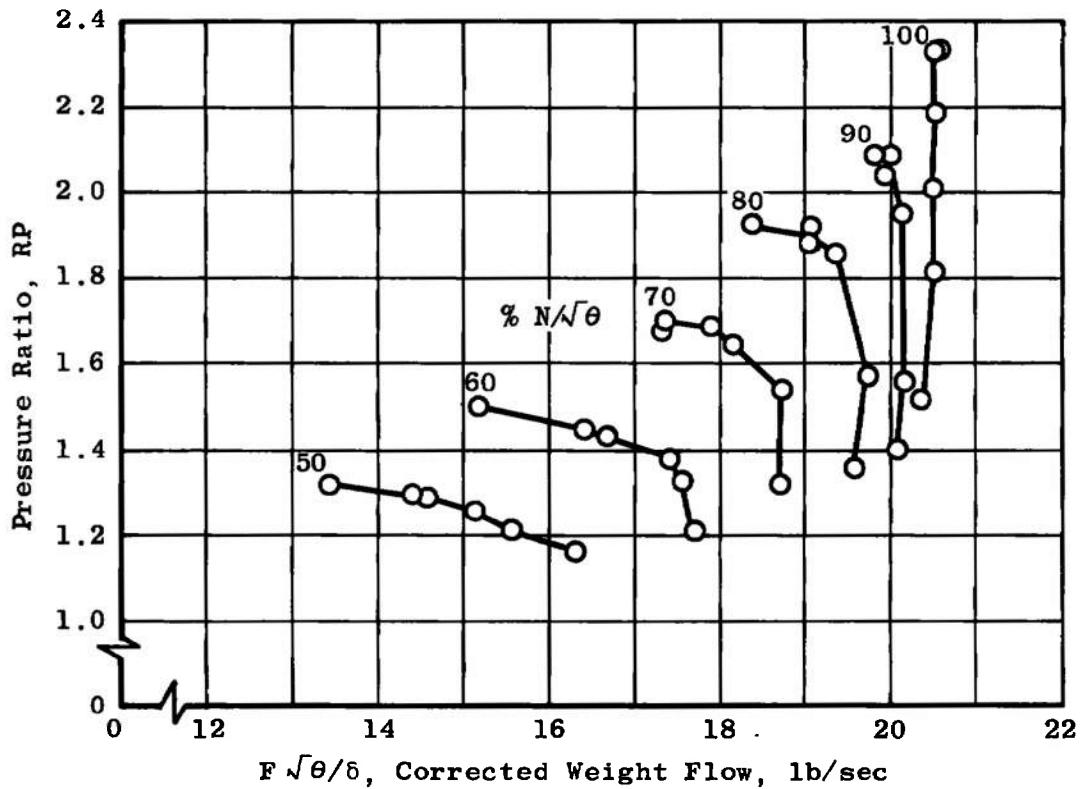
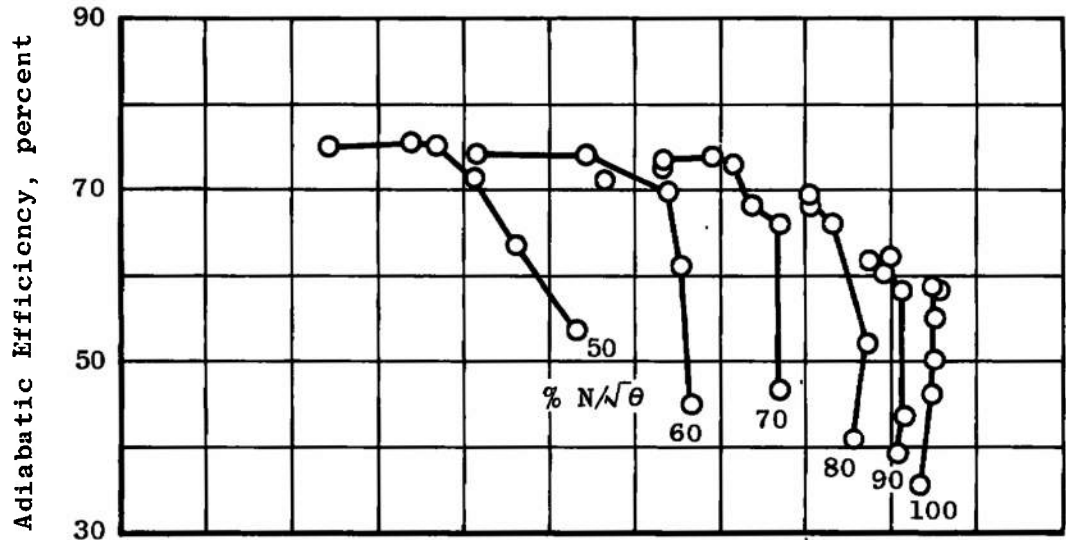
Fig. IV-2 Configuration 2

- a. Compressor Performance Characteristics Based on Equivalent Weight Flow
- b. Compressor Performance Characteristics Based on Weight Flow Ratio
- c. Inlet Parameters
- d. Exit Parameters
- e. Adiabatic Efficiency and Pressure Ratio
- f. Exit Specific Mass Flow and Enthalpy Rise

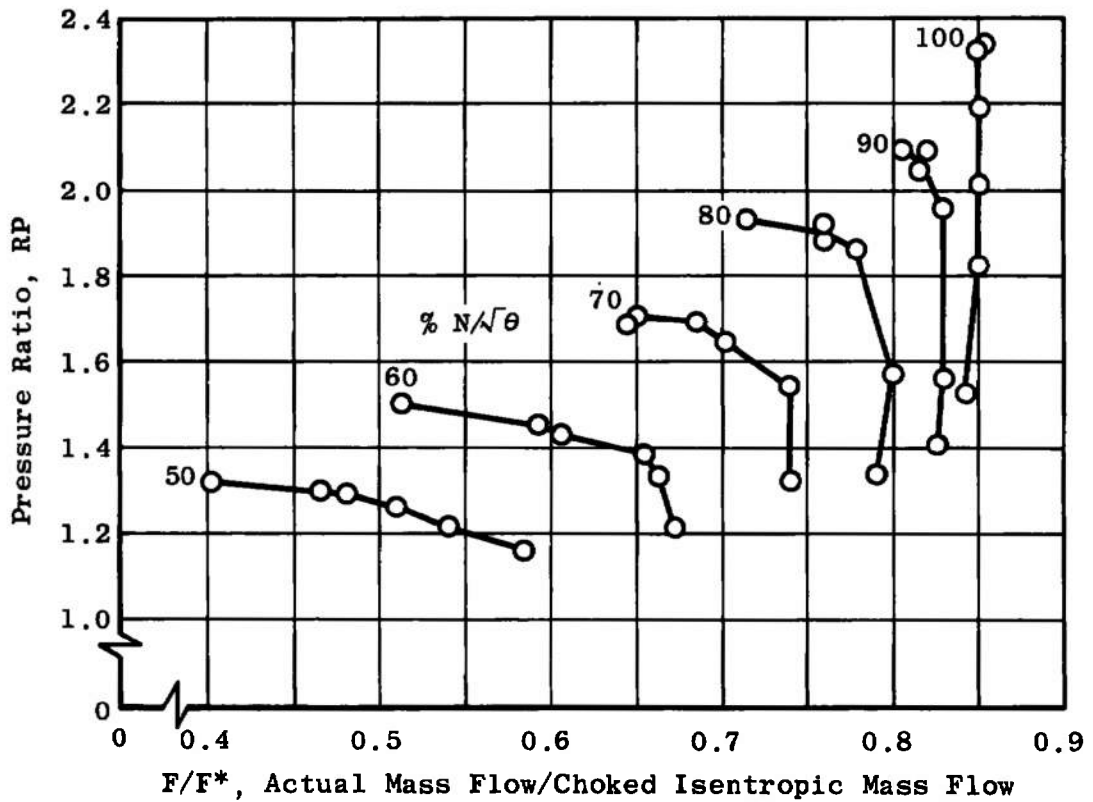
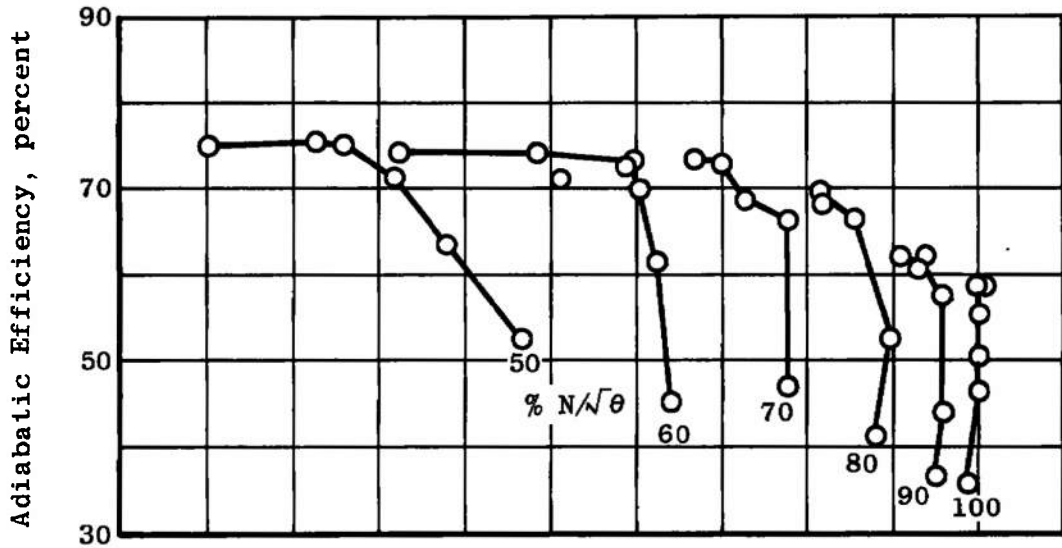
TABLES

IV-I. Configuration 1

IV-II. Configuration 2

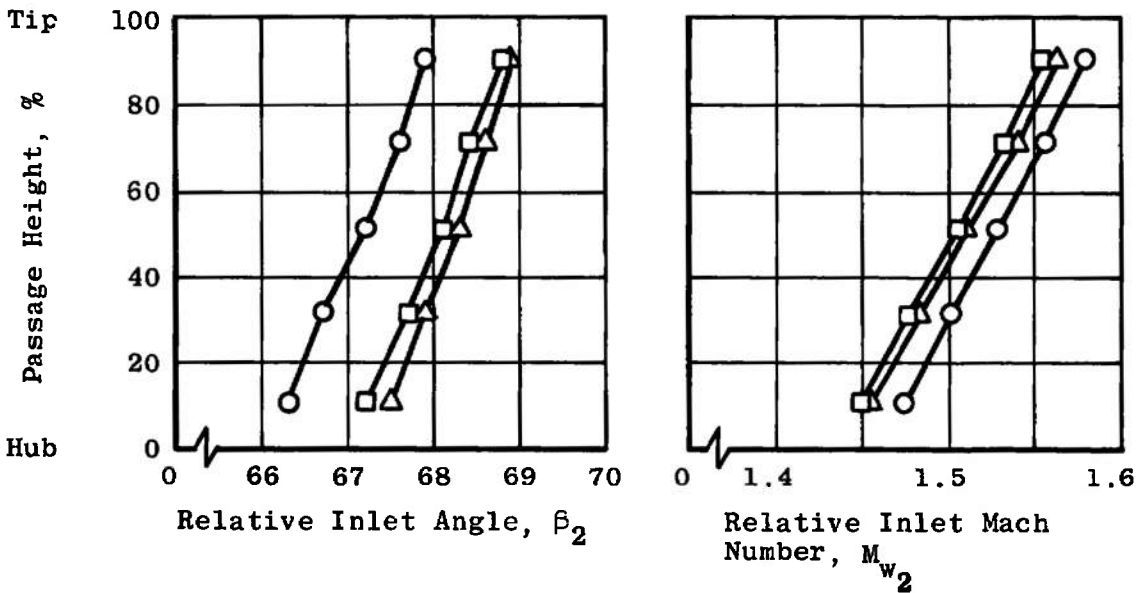
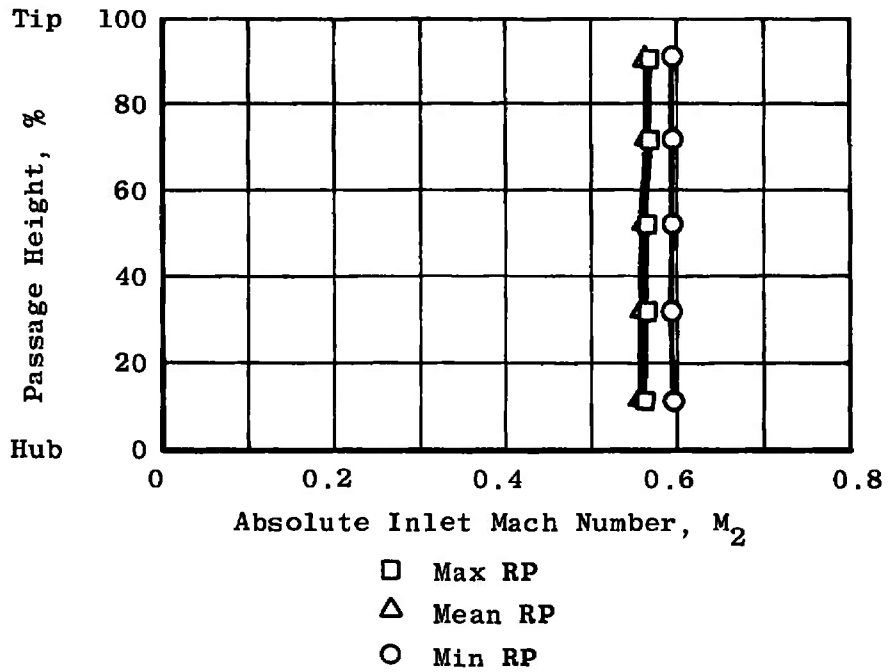


a. Compressor Performance Characteristics Based on Equivalent Weight Flow
 Fig. IV-1 Configuration 1

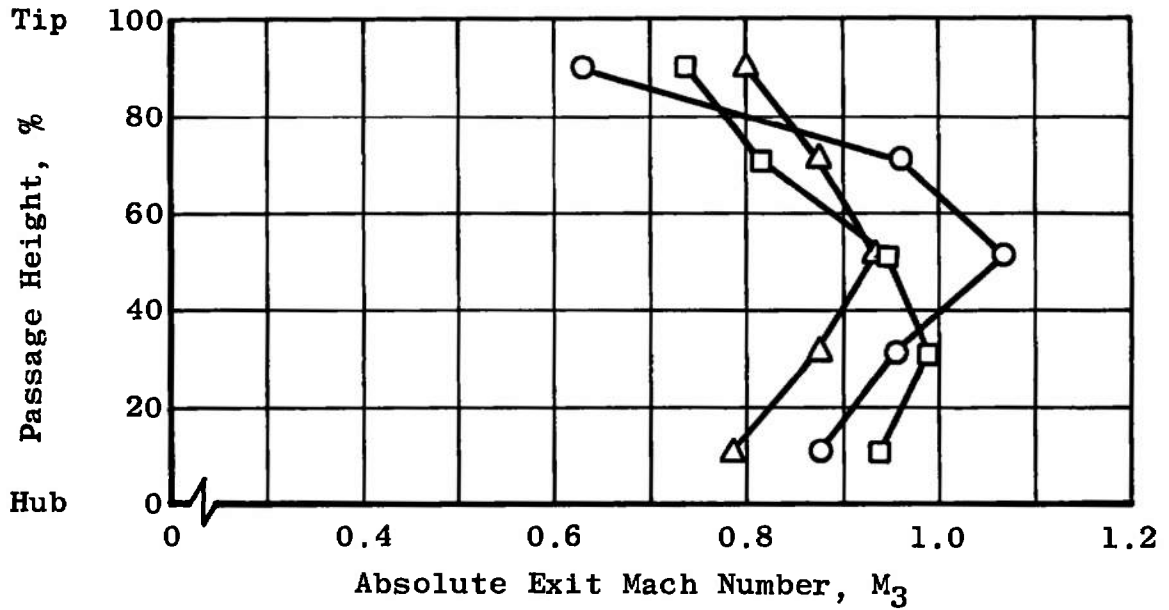


b. Compressor Performance Characteristics Based on Weight Flow Ratio

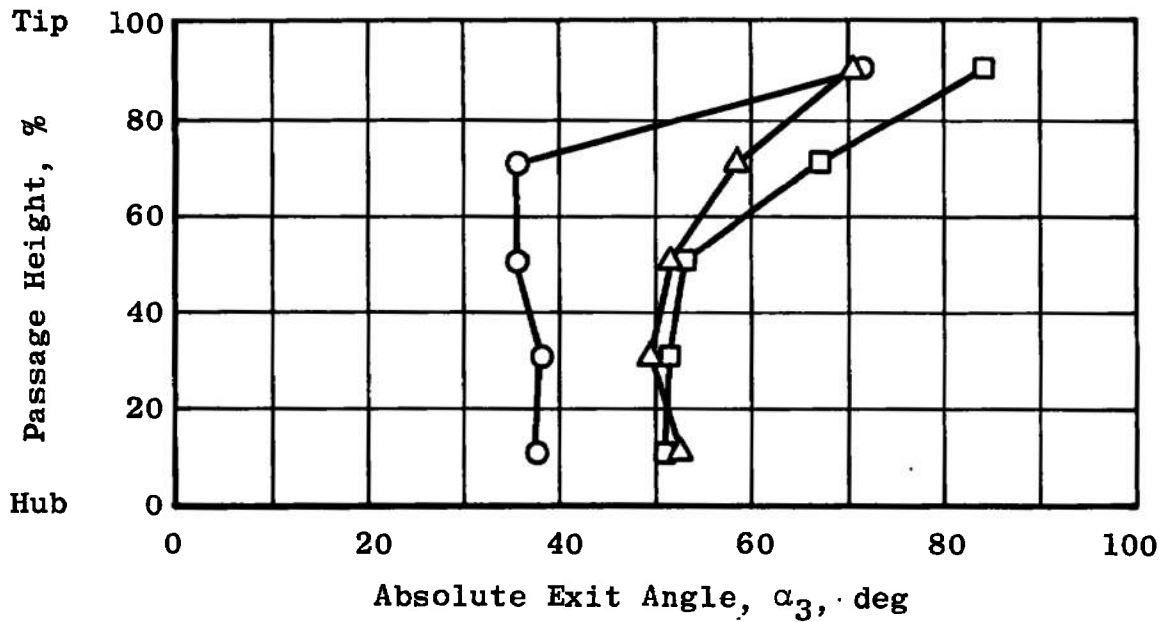
Fig. IV-1 Continued



c. Inlet Parameters, 100% $N/\sqrt{\theta}$
 Fig. IV-1 Continued

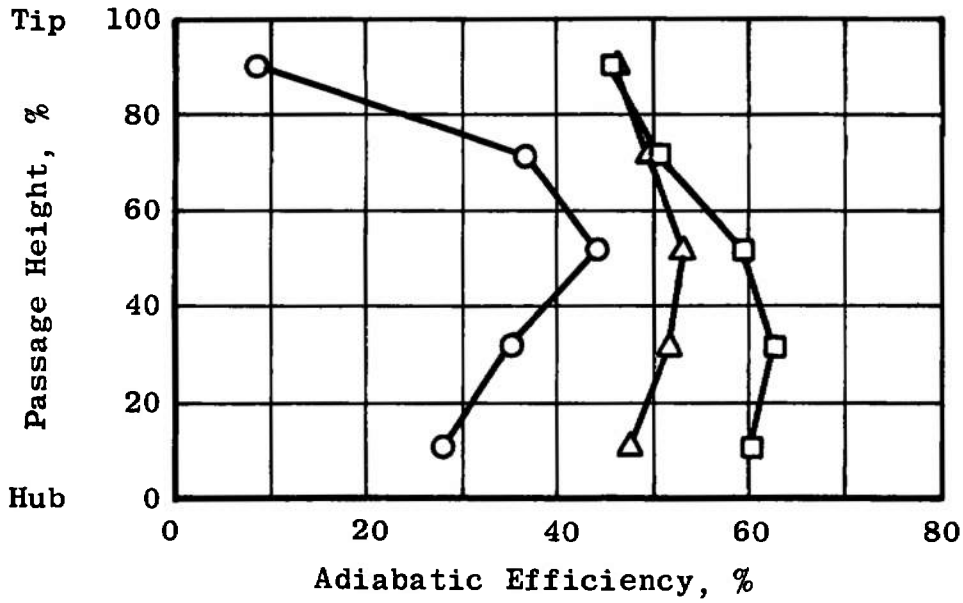


- Max RP
- △ Mean RP
- Min RP

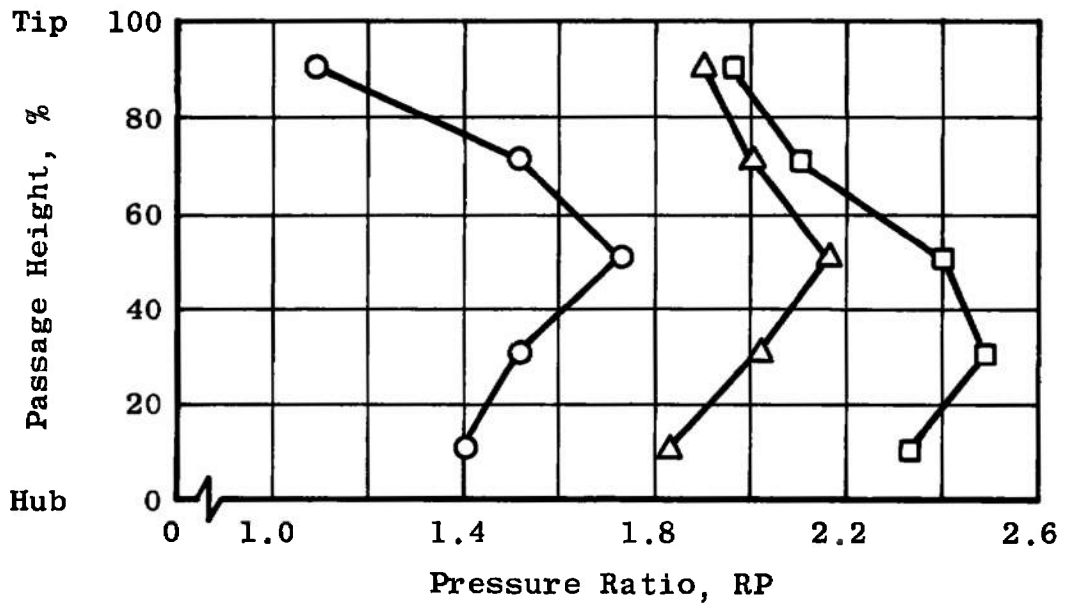


d. Exit Parameters, 100% $N/\sqrt{\theta}$

Fig. IV-1 Continued

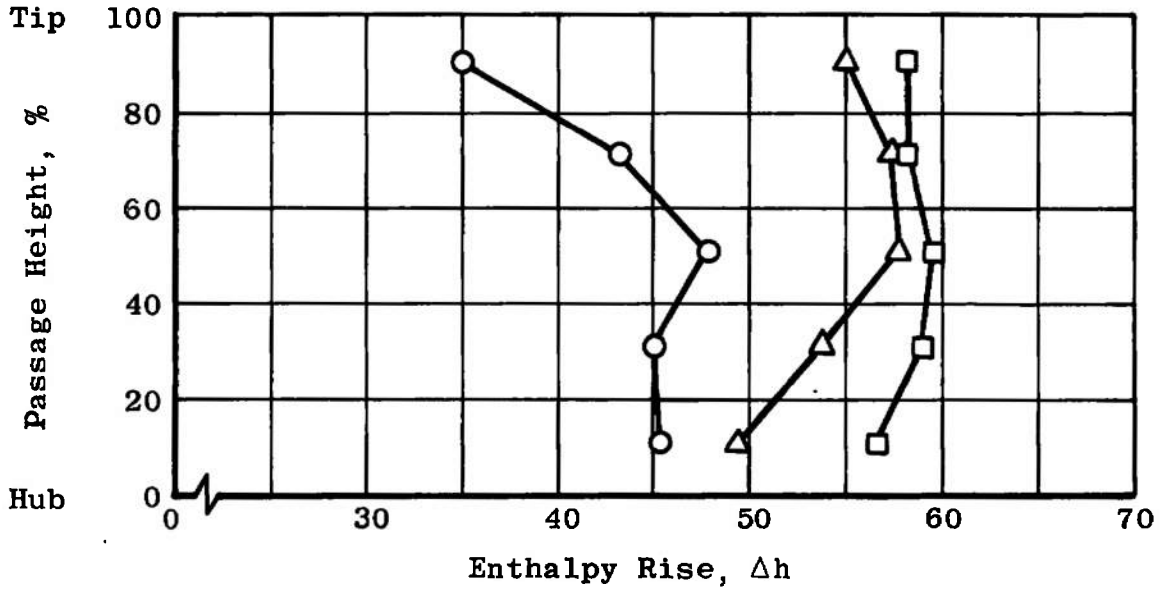
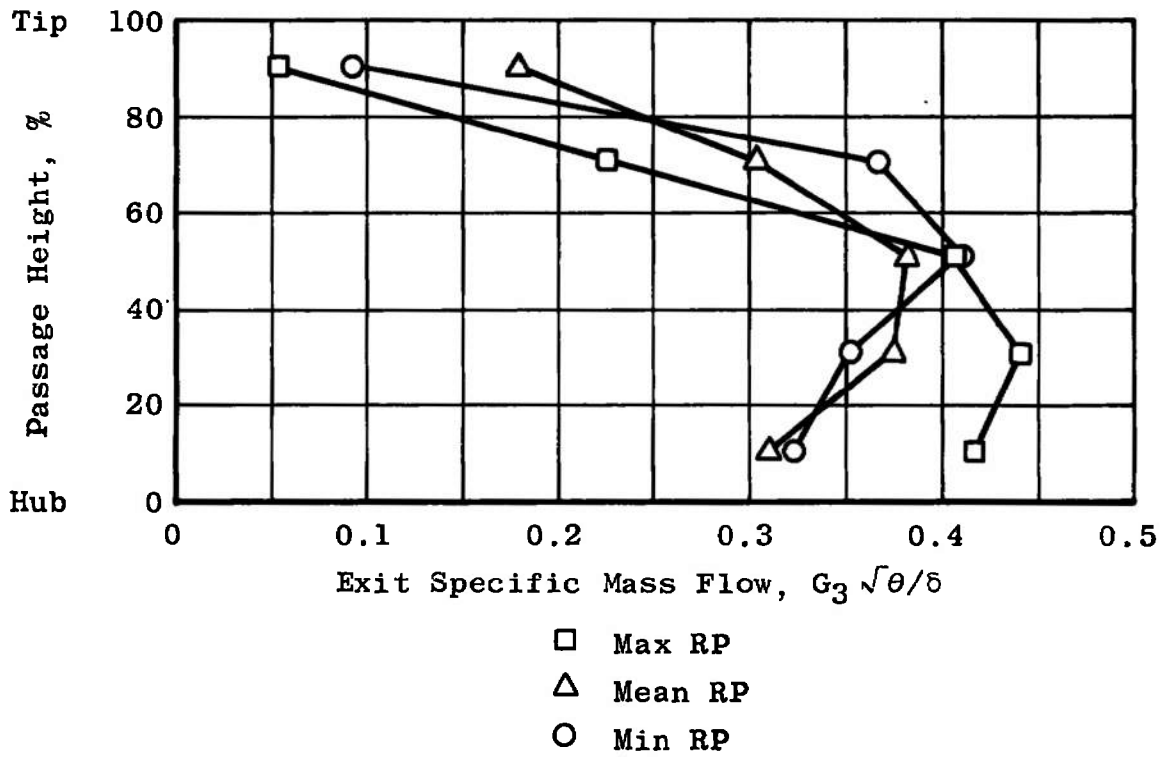


- Max RP
- △ Mean RP
- Min RP

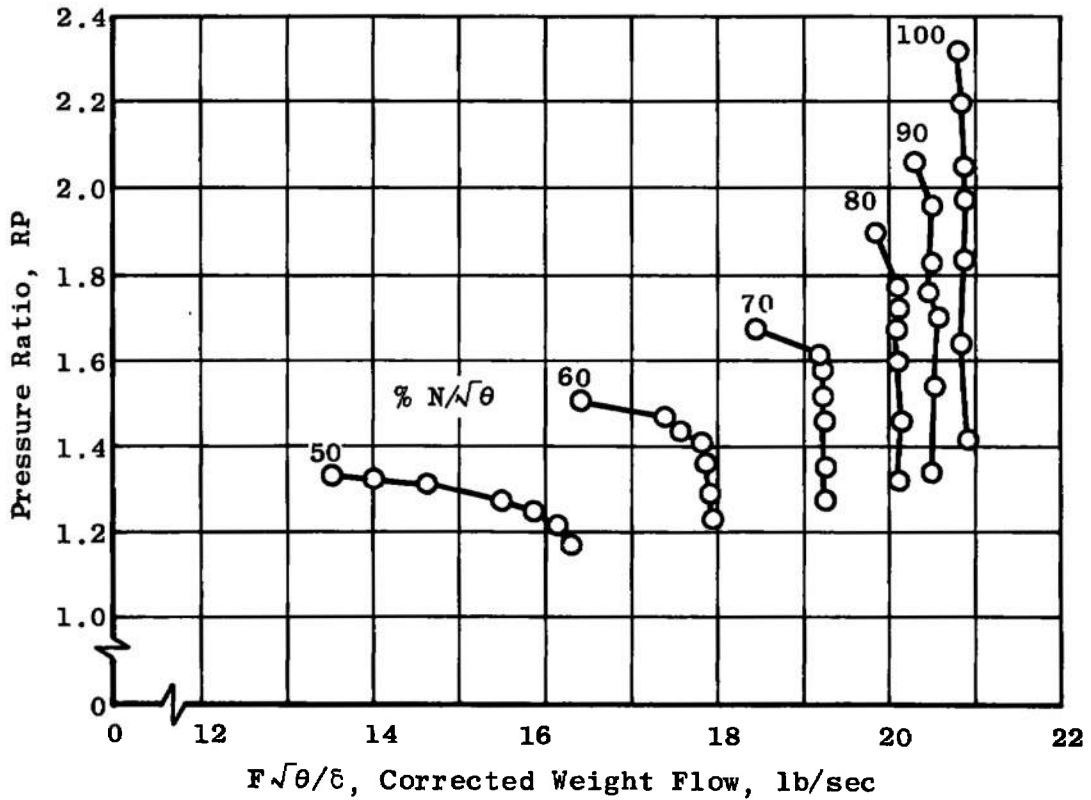
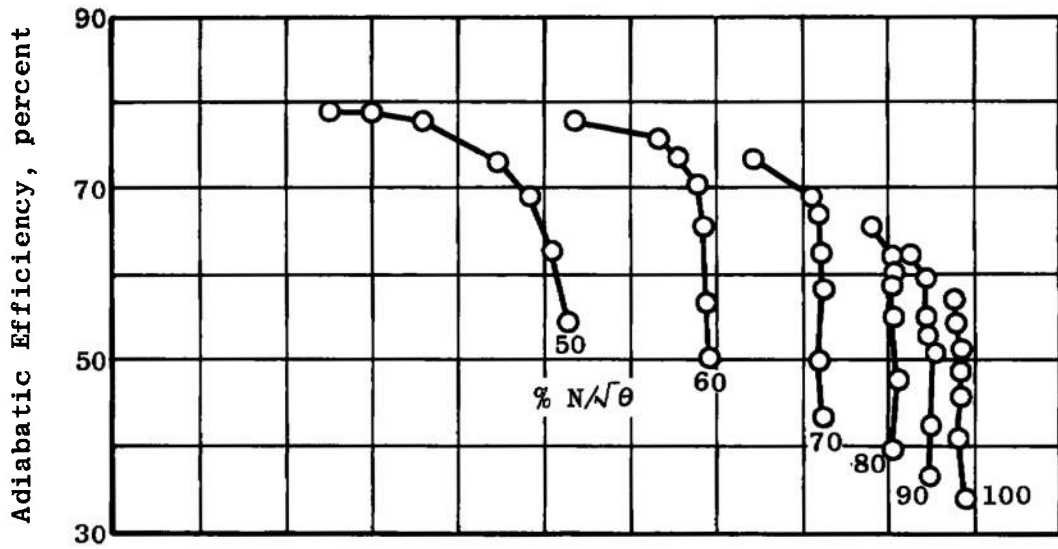


e. Adiabatic Efficiency and Pressure Ratio, 100% $N/\sqrt{\theta}$

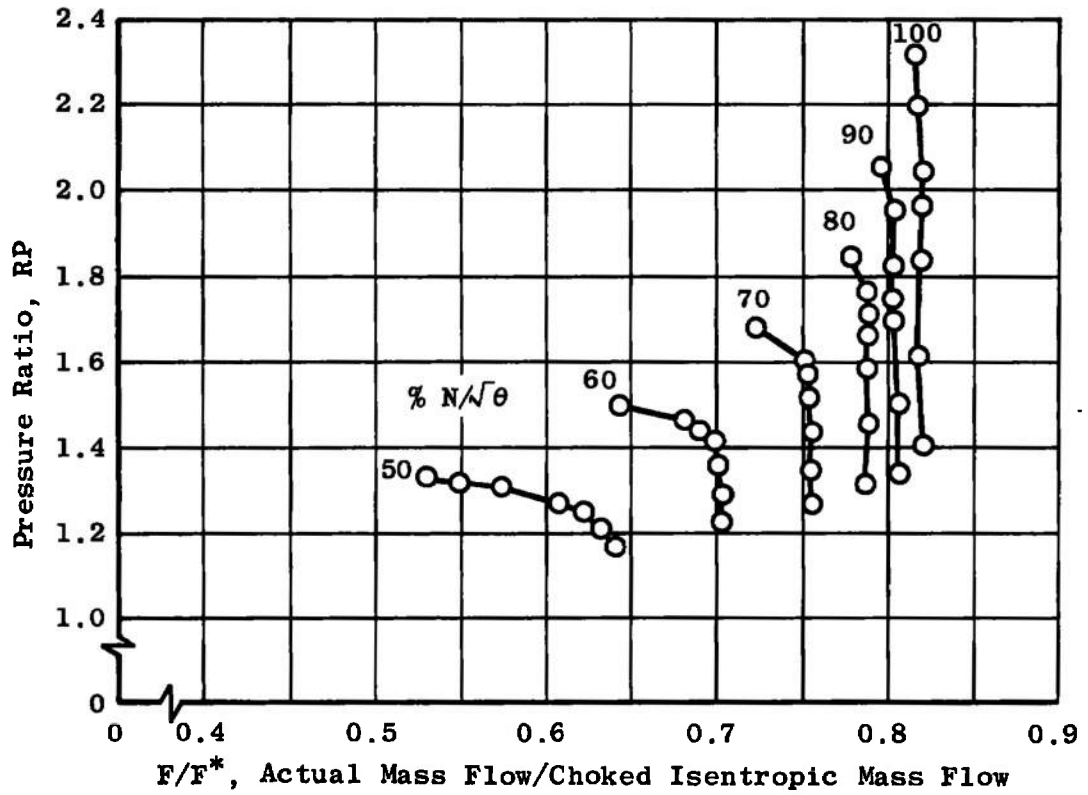
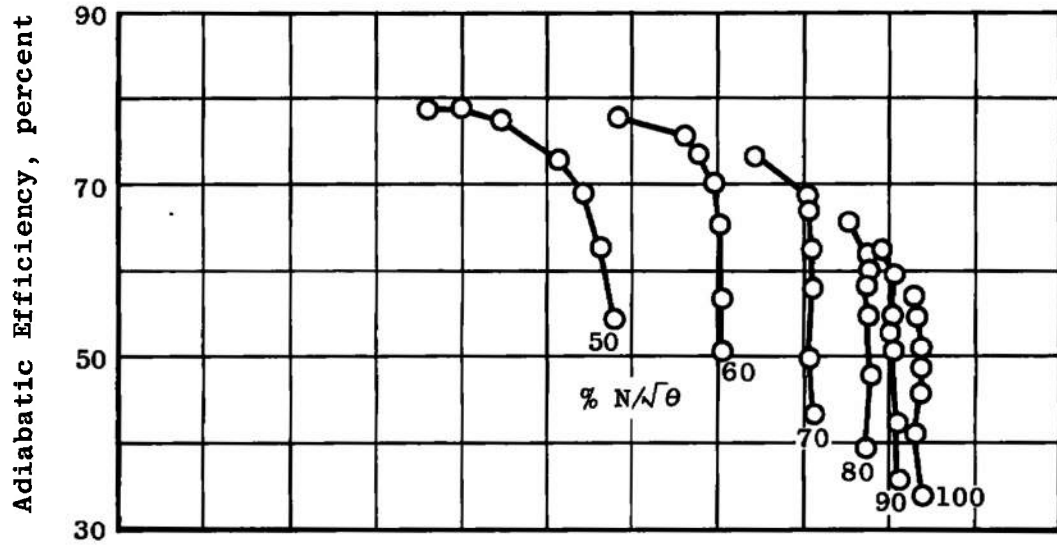
Fig. IV-1 Continued



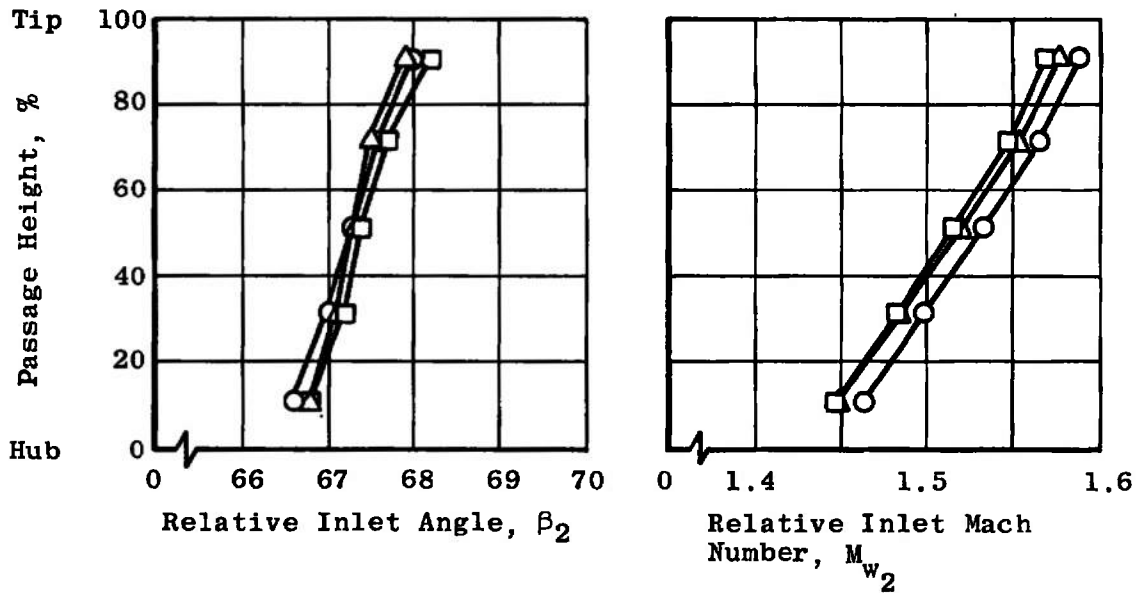
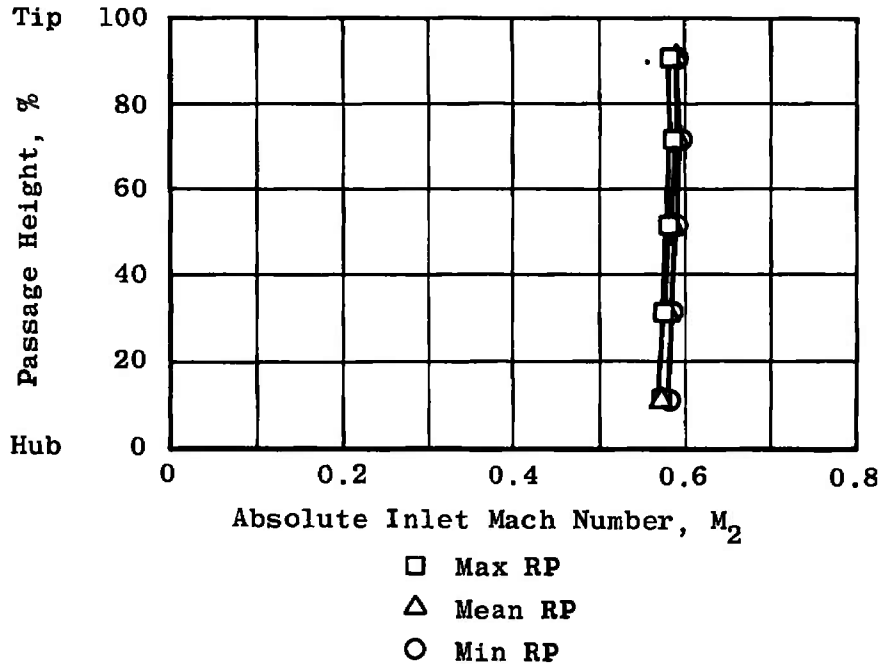
f. Exit Specific Mass Flow and Enthalpy Rise, 100% $N/\sqrt{\theta}$
 Fig. IV-1 Concluded



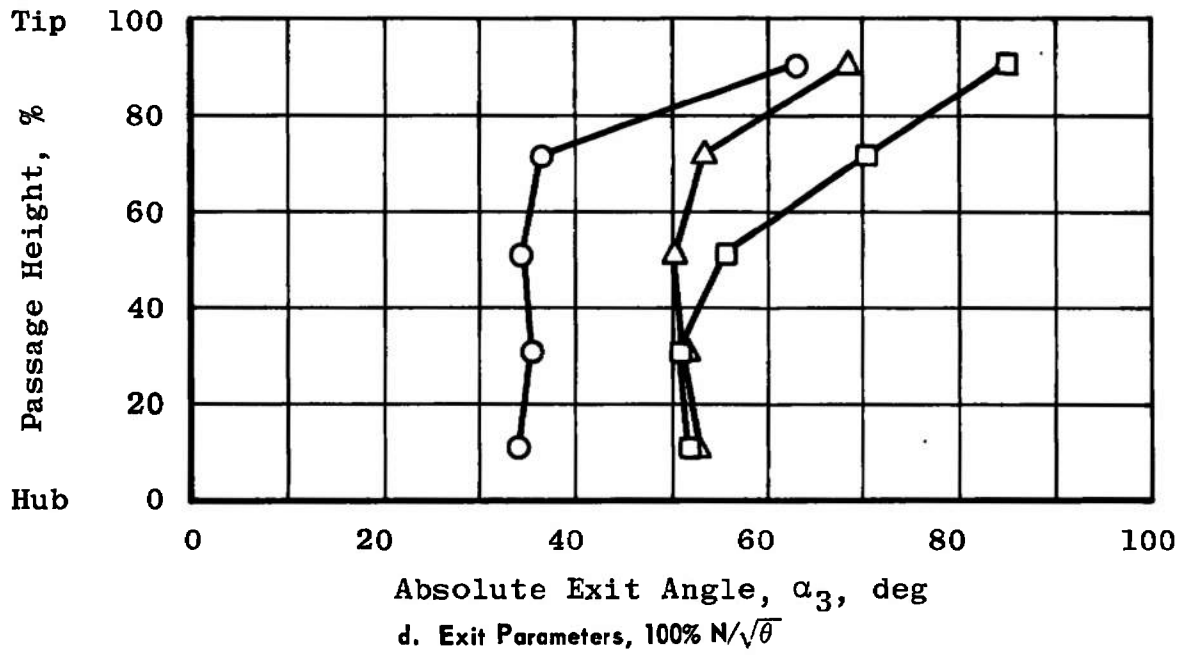
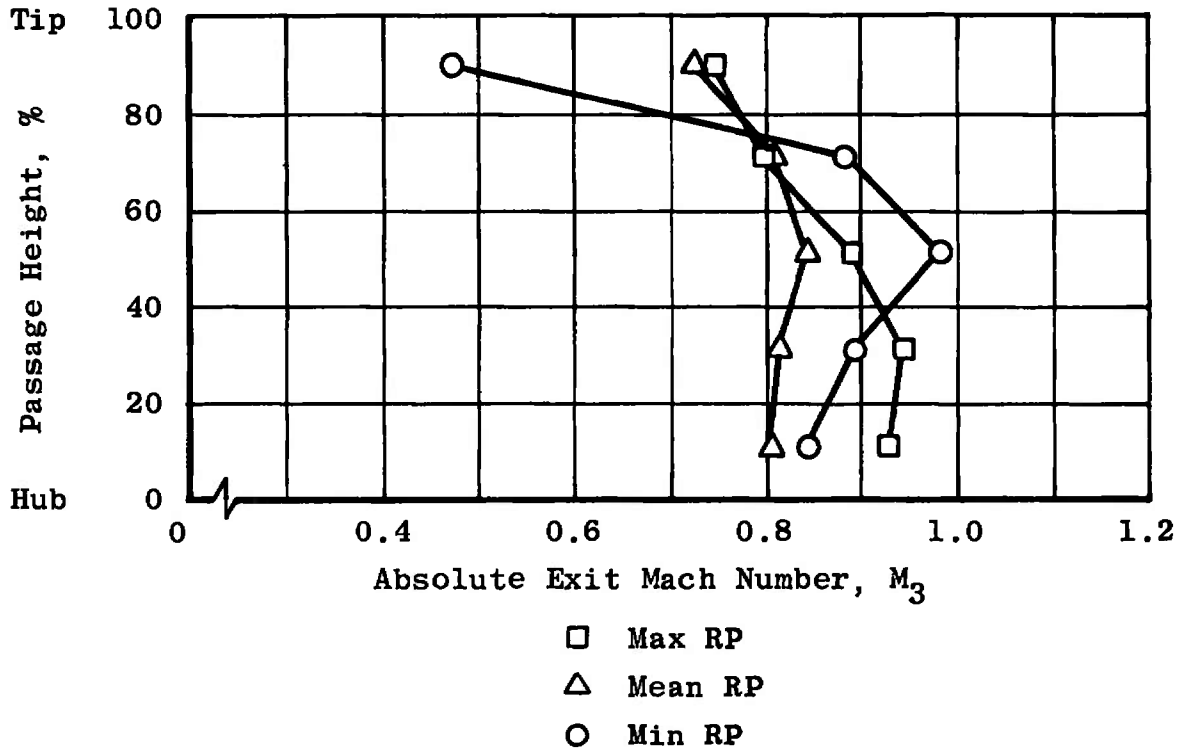
a. Compressor Performance Characteristics Based on Equivalent Weight Flow
 Fig. IV-2 Configuration 2



b. Compressor Performance Characteristics Based on Weight Flow Ratio
 Fig. IV-2 Continued

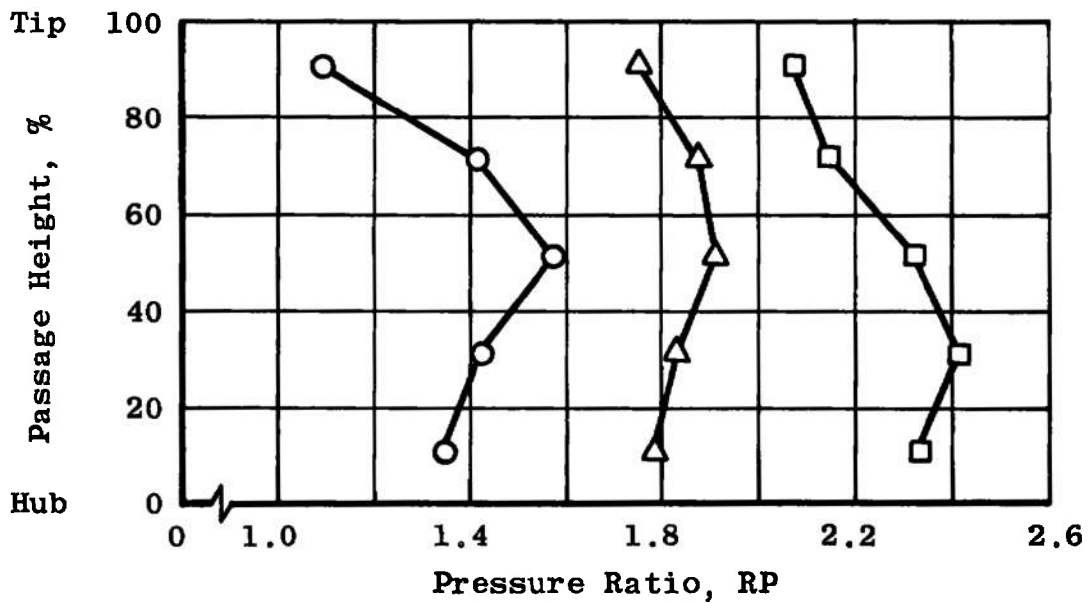
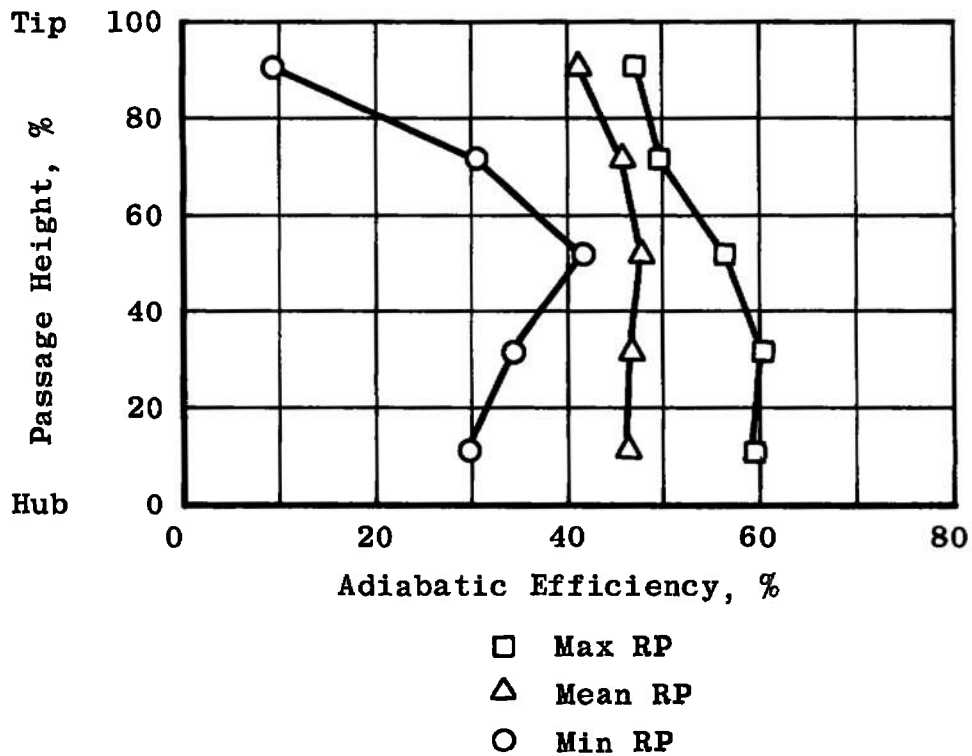


c. Inlet Parameters, 100% $N/\sqrt{\theta}$
Fig. IV-2 Continued

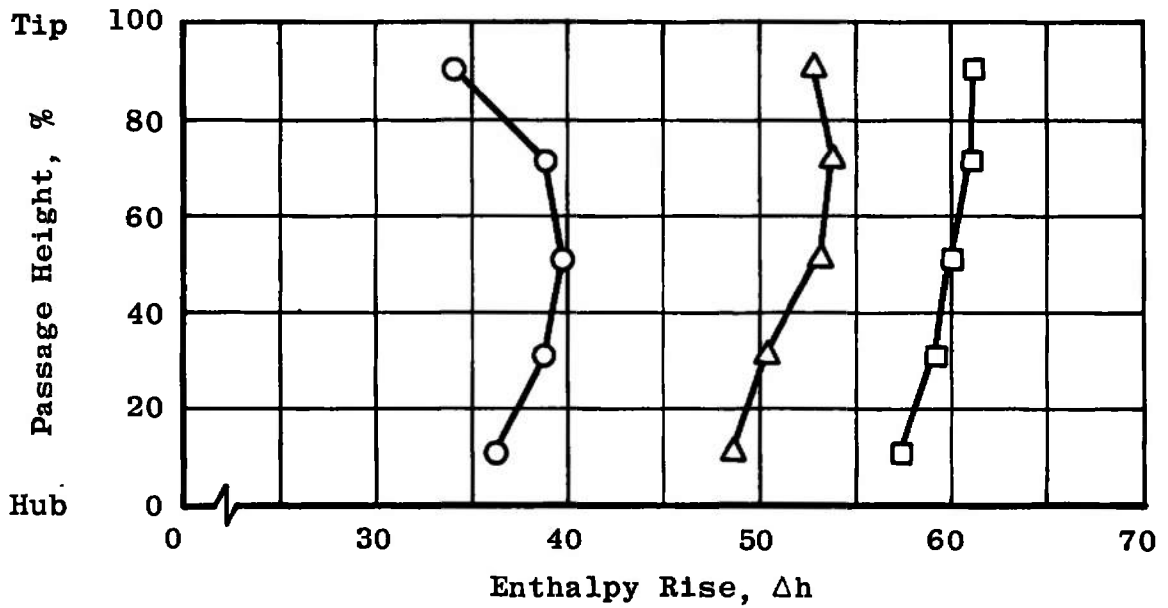
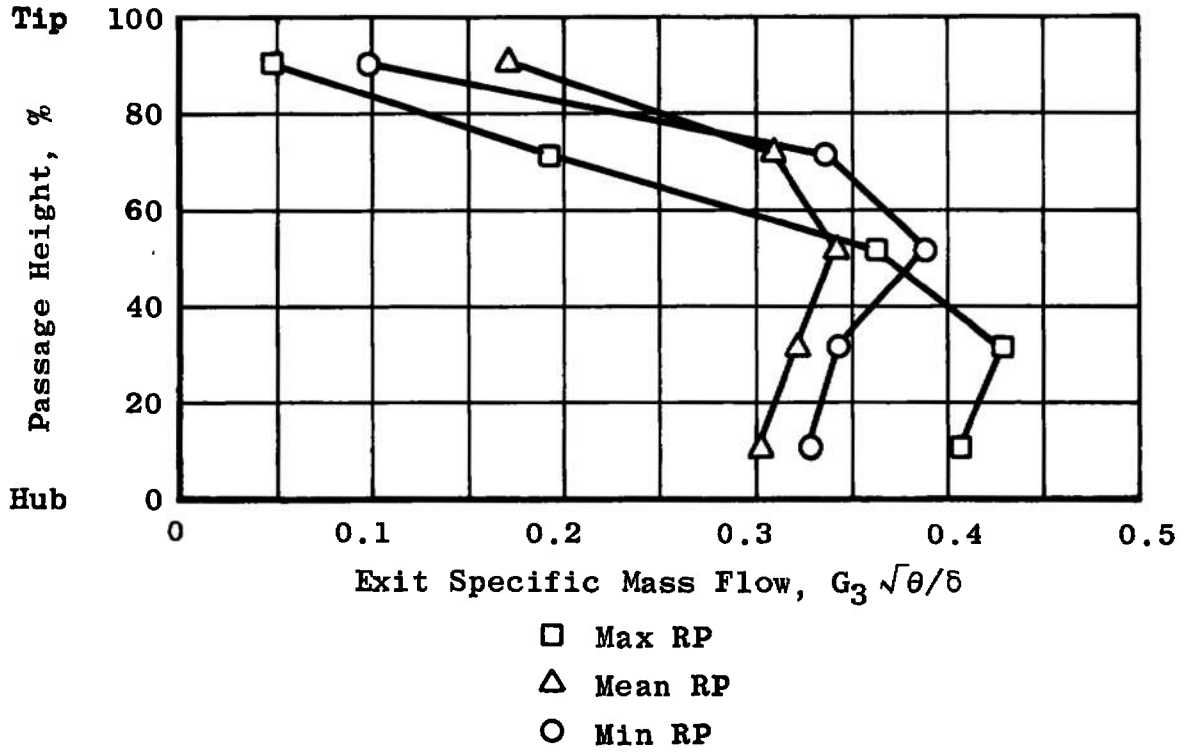


d. Exit Parameters, $100\% N/\sqrt{\theta}$

Fig. IV-2 Continued



e. Adiabatic Efficiency and Pressure Ratio, 100% $N/\sqrt{\theta}$
 Fig. IV-2 Continued



t. Exit Specific Mass Flow and Enthalpy Rise, 100% $N\sqrt{\theta}$

Fig. IV-2 Concluded

TABLE IV-1
CONFIGURATION 1

| RP | Area Centers | M ₂ | β ₂ deg | M _{w2} | η % | RP | M ₃ | α ₃ deg | G ₃ $\frac{\sqrt{\theta}}{\delta}$ | ΔH/θ |
|----|--------------|----------------|--------------------|-----------------|-----|----|----------------|--------------------|---|------|
|----|--------------|----------------|--------------------|-----------------|-----|----|----------------|--------------------|---|------|

100% N

| | | | | | | | | | | |
|---------|---|-------|------|-------|------|------|-------|------|-------|-------|
| MAXIMUM | 1 | 0.563 | 68.8 | 1.554 | 45.5 | 1.96 | 0.738 | 84.1 | 0.054 | 58.12 |
| | 2 | 0.566 | 68.4 | 1.532 | 50.3 | 2.10 | 0.813 | 67.0 | 0.225 | 58.23 |
| | 3 | 0.561 | 68.1 | 1.505 | 59.2 | 2.40 | 0.948 | 53.1 | 0.406 | 59.58 |
| | 4 | 0.561 | 67.7 | 1.476 | 62.7 | 2.49 | 0.989 | 51.3 | 0.441 | 58.93 |
| | 5 | 0.560 | 67.2 | 1.449 | 60.0 | 2.33 | 0.938 | 51.0 | 0.416 | 56.60 |
| MEAN | 1 | 0.562 | 68.9 | 1.563 | 45.6 | 1.90 | 0.799 | 70.2 | 0.178 | 55.03 |
| | 2 | 0.563 | 68.6 | 1.540 | 49.2 | 2.05 | 0.877 | 58.2 | 0.303 | 57.44 |
| | 3 | 0.558 | 68.3 | 1.511 | 53.0 | 2.16 | 0.932 | 51.3 | 0.382 | 57.77 |
| | 4 | 0.558 | 67.9 | 1.483 | 51.6 | 2.02 | 0.877 | 49.2 | 0.375 | 53.77 |
| | 5 | 0.557 | 67.5 | 1.455 | 47.3 | 1.83 | 0.783 | 52.4 | 0.310 | 49.45 |
| MINIMUM | 1 | 0.593 | 67.9 | 1.579 | 8.7 | 1.09 | 0.627 | 71.5 | 0.091 | 34.96 |
| | 2 | 0.594 | 67.6 | 1.556 | 36.4 | 1.52 | 0.960 | 35.4 | 0.366 | 43.07 |
| | 3 | 0.594 | 67.2 | 1.528 | 44.1 | 1.73 | 1.069 | 35.5 | 0.409 | 47.81 |
| | 4 | 0.591 | 66.7 | 1.501 | 35.0 | 1.52 | 0.953 | 38.0 | 0.352 | 44.99 |
| | 5 | 0.593 | 66.3 | 1.474 | 27.9 | 1.40 | 0.877 | 37.5 | 0.323 | 45.35 |

90% N

| | | | | | | | | | | |
|---------|---|-------|------|-------|------|------|-------|------|-------|-------|
| MAXIMUM | 1 | 0.548 | 67.3 | 1.421 | 58.0 | 2.09 | 0.772 | 69.9 | 0.199 | 50.18 |
| | 2 | 0.554 | 66.7 | 1.404 | 59.2 | 2.11 | 0.791 | 64.5 | 0.253 | 49.89 |
| | 3 | 0.557 | 66.2 | 1.382 | 63.0 | 2.15 | 0.818 | 57.9 | 0.323 | 48.10 |
| | 4 | 0.562 | 65.6 | 1.360 | 65.7 | 2.13 | 0.820 | 54.0 | 0.357 | 45.66 |
| | 5 | 0.567 | 64.9 | 1.339 | 62.0 | 1.99 | 0.760 | 55.2 | 0.318 | 43.49 |
| MEAN | 1 | 0.580 | 66.3 | 1.441 | 51.9 | 1.81 | 0.703 | 68.3 | 0.180 | 44.14 |
| | 2 | 0.582 | 65.8 | 1.421 | 56.1 | 1.94 | 0.792 | 58.0 | 0.291 | 46.69 |
| | 3 | 0.581 | 65.4 | 1.397 | 60.6 | 2.09 | 0.864 | 54.3 | 0.350 | 48.00 |
| | 4 | 0.581 | 65.0 | 1.372 | 58.6 | 1.97 | 0.814 | 52.0 | 0.345 | 45.28 |
| | 5 | 0.580 | 64.5 | 1.348 | 56.2 | 1.84 | 0.752 | 52.5 | 0.313 | 42.01 |
| MINIMUM | 1 | 0.581 | 66.2 | 1.440 | 11.4 | 1.09 | 0.568 | 54.5 | 0.160 | 26.40 |
| | 2 | 0.578 | 65.9 | 1.416 | 44.4 | 1.51 | 0.920 | 31.2 | 0.391 | 35.07 |
| | 3 | 0.576 | 65.6 | 1.392 | 41.8 | 1.48 | 0.901 | 36.0 | 0.361 | 35.48 |
| | 4 | 0.572 | 65.2 | 1.365 | 34.7 | 1.38 | 0.826 | 36.3 | 0.328 | 34.08 |
| | 5 | 0.570 | 64.8 | 1.340 | 29.2 | 1.33 | 0.790 | 37.4 | 0.307 | 36.03 |

TABLE IV-1 (Continued)

| RP | Area Centers | M_2 | β_2 deg | M_{w2} | η % | RP | M_3 | α_3 deg | $G_3 \frac{\sqrt{\theta}}{\delta}$ | $\Delta H/\theta$ |
|----|--------------|-------|---------------|----------|----------|----|-------|----------------|------------------------------------|-------------------|
|----|--------------|-------|---------------|----------|----------|----|-------|----------------|------------------------------------|-------------------|

80% N

| | | | | | | | | | | |
|---------|---|-------|------|-------|------|------|-------|------|-------|-------|
| MAXIMUM | 1 | 0.508 | 66.4 | 1.267 | 64.0 | 1.96 | 0.736 | 66.7 | 0.206 | 41.09 |
| | 2 | 0.517 | 65.6 | 1.253 | 64.9 | 1.96 | 0.743 | 62.9 | 0.301 | 40.57 |
| | 3 | 0.523 | 65.0 | 1.235 | 71.2 | 1.97 | 0.758 | 58.3 | 0.320 | 37.46 |
| | 4 | 0.528 | 64.3 | 1.217 | 72.6 | 1.93 | 0.739 | 55.2 | 0.360 | 35.25 |
| | 5 | 0.534 | 63.5 | 1.199 | 68.0 | 1.80 | 0.670 | 60.1 | 0.217 | 33.38 |
| MEAN | 1 | 0.562 | 64.3 | 1.297 | 43.3 | 1.47 | 0.633 | 62.1 | 0.182 | 33.49 |
| | 2 | 0.562 | 63.9 | 1.278 | 50.4 | 1.61 | 0.745 | 48.1 | 0.306 | 36.20 |
| | 3 | 0.560 | 63.5 | 1.257 | 56.8 | 1.67 | 0.785 | 47.4 | 0.329 | 33.07 |
| | 4 | 0.558 | 63.1 | 1.234 | 53.9 | 1.55 | 0.716 | 44.5 | 0.315 | 30.98 |
| | 5 | 0.558 | 62.6 | 1.213 | 52.0 | 1.47 | 0.661 | 44.2 | 0.291 | 27.95 |
| MINIMUM | 1 | 0.558 | 64.5 | 1.299 | 38.0 | 1.34 | 0.695 | 43.2 | 0.276 | 28.89 |
| | 2 | 0.558 | 64.1 | 1.280 | 37.6 | 1.36 | 0.706 | 40.0 | 0.294 | 30.01 |
| | 3 | 0.558 | 63.7 | 1.259 | 39.0 | 1.35 | 0.705 | 38.0 | 0.302 | 28.72 |
| | 4 | 0.557 | 63.2 | 1.237 | 38.6 | 1.32 | 0.680 | 34.3 | 0.307 | 26.68 |
| | 5 | 0.554 | 62.8 | 1.214 | 27.8 | 1.21 | 0.572 | 43.2 | 0.226 | 24.89 |

70% N

| | | | | | | | | | | |
|---------|---|-------|------|-------|------|------|-------|------|-------|-------|
| MAXIMUM | 1 | 0.428 | 67.0 | 1.096 | 69.0 | 1.73 | 0.649 | 63.8 | 0.207 | 30.60 |
| | 2 | 0.438 | 66.2 | 1.084 | 70.7 | 1.74 | 0.662 | 60.2 | 0.237 | 30.18 |
| | 3 | 0.444 | 65.5 | 1.069 | 76.4 | 1.74 | 0.670 | 56.5 | 0.267 | 28.00 |
| | 4 | 0.452 | 64.6 | 1.055 | 77.3 | 1.70 | 0.647 | 54.0 | 0.274 | 26.36 |
| | 5 | 0.460 | 63.8 | 1.041 | 72.1 | 1.60 | 0.580 | 59.3 | 0.224 | 24.88 |
| MEAN | 1 | 0.517 | 63.1 | 1.143 | 61.0 | 1.51 | 0.598 | 52.5 | 0.241 | 24.96 |
| | 2 | 0.517 | 62.7 | 1.127 | 65.2 | 1.60 | 0.674 | 49.0 | 0.293 | 26.87 |
| | 3 | 0.516 | 62.3 | 1.108 | 66.9 | 1.59 | 0.671 | 48.7 | 0.294 | 24.91 |
| | 4 | 0.514 | 61.8 | 1.089 | 69.2 | 1.54 | 0.639 | 44.5 | 0.301 | 23.51 |
| | 5 | 0.512 | 61.4 | 1.070 | 63.2 | 1.42 | 0.547 | 50.5 | 0.228 | 21.99 |
| MINIMUM | 1 | 0.513 | 63.2 | 1.137 | 47.4 | 1.36 | 0.659 | 45.6 | 0.265 | 24.06 |
| | 2 | 0.514 | 62.7 | 1.121 | 47.2 | 1.37 | 0.670 | 41.3 | 0.288 | 24.68 |
| | 3 | 0.512 | 62.3 | 1.103 | 48.5 | 1.36 | 0.662 | 42.2 | 0.281 | 23.25 |
| | 4 | 0.512 | 61.8 | 1.083 | 49.9 | 1.31 | 0.628 | 36.7 | 0.290 | 20.10 |
| | 5 | 0.511 | 61.3 | 1.064 | 37.0 | 1.20 | 0.513 | 40.0 | 0.224 | 17.95 |

TABLE IV-1 (Continued)

| RP | Area Centers | M ₂ | β ₂ deg | M _{w2} | η% | RP | M ₃ | α ₃ deg | G ₃ $\frac{\sqrt{\theta}}{\delta}$ | ΔH/θ |
|----|--------------|----------------|--------------------|-----------------|----|----|----------------|--------------------|---|------|
|----|--------------|----------------|--------------------|-----------------|----|----|----------------|--------------------|---|------|

60% N

| | | | | | | | | | | |
|---------|---|-------|------|-------|------|------|-------|------|-------|-------|
| MAXIMUM | 1 | 0.361 | 67.2 | 0.932 | 71.2 | 1.51 | 0.573 | 61.5 | 0.190 | 21.74 |
| | 2 | 0.366 | 66.6 | 0.920 | 73.2 | 1.52 | 0.588 | 58.2 | 0.236 | 21.62 |
| | 3 | 0.370 | 65.9 | 0.907 | 78.5 | 1.52 | 0.593 | 55.7 | 0.236 | 20.16 |
| | 4 | 0.372 | 65.3 | 0.892 | 76.4 | 1.49 | 0.569 | 53.6 | 0.252 | 19.57 |
| | 5 | 0.375 | 64.7 | 0.877 | 72.0 | 1.43 | 0.519 | 57.0 | 0.185 | 18.57 |
| MEAN | 1 | 0.411 | 64.5 | 0.956 | 67.1 | 1.37 | 0.529 | 48.7 | 0.226 | 17.48 |
| | 2 | 0.416 | 63.9 | 0.944 | 70.6 | 1.43 | 0.591 | 47.2 | 0.259 | 18.95 |
| | 3 | 0.413 | 63.6 | 0.927 | 73.0 | 1.41 | 0.581 | 46.2 | 0.260 | 17.72 |
| | 4 | 0.417 | 62.8 | 0.914 | 72.9 | 1.38 | 0.551 | 41.9 | 0.264 | 16.34 |
| | 5 | 0.418 | 62.3 | 0.898 | 62.1 | 1.30 | 0.467 | 50.2 | 0.191 | 15.42 |
| MINIMUM | 1 | 0.455 | 62.3 | 0.979 | 44.8 | 1.22 | 0.556 | 36.5 | 0.255 | 16.55 |
| | 2 | 0.456 | 61.8 | 0.965 | 45.0 | 1.23 | 0.569 | 37.0 | 0.258 | 17.13 |
| | 3 | 0.454 | 61.4 | 0.949 | 47.4 | 1.24 | 0.574 | 39.4 | 0.252 | 16.37 |
| | 4 | 0.456 | 60.8 | 0.934 | 46.8 | 1.19 | 0.526 | 34.6 | 0.247 | 13.67 |
| | 5 | 0.456 | 60.2 | 0.918 | 38.3 | 1.14 | 0.460 | 37.6 | 0.207 | 12.19 |

50% N

| | | | | | | | | | | |
|---------|---|-------|------|-------|------|------|-------|------|-------|-------|
| MAXIMUM | 1 | 0.296 | 67.5 | 0.772 | 70.0 | 1.32 | 0.476 | 64.0 | 0.140 | 14.58 |
| | 2 | 0.304 | 66.5 | 0.764 | 73.6 | 1.34 | 0.504 | 57.0 | 0.209 | 14.74 |
| | 3 | 0.308 | 65.8 | 0.753 | 79.1 | 1.34 | 0.507 | 53.7 | 0.201 | 13.72 |
| | 4 | 0.310 | 65.2 | 0.740 | 78.0 | 1.31 | 0.480 | 50.5 | 0.222 | 12.94 |
| | 5 | 0.317 | 64.3 | 0.730 | 72.5 | 1.27 | 0.428 | 53.8 | 0.154 | 12.17 |
| MEAN | 1 | 0.350 | 63.8 | 0.801 | 70.2 | 1.26 | 0.475 | 43.4 | 0.216 | 12.11 |
| | 2 | 0.357 | 63.1 | 0.791 | 75.2 | 1.29 | 0.506 | 44.0 | 0.228 | 12.30 |
| | 3 | 0.361 | 62.5 | 0.780 | 73.6 | 1.27 | 0.492 | 45.7 | 0.215 | 12.03 |
| | 4 | 0.359 | 62.0 | 0.766 | 72.6 | 1.25 | 0.460 | 38.1 | 0.226 | 11.07 |
| | 5 | 0.357 | 61.6 | 0.752 | 65.0 | 1.20 | 0.394 | 47.4 | 0.168 | 10.21 |
| MINIMUM | 1 | 0.396 | 61.2 | 0.822 | 54.8 | 1.17 | 0.474 | 36.8 | 0.221 | 10.21 |
| | 2 | 0.397 | 60.7 | 0.811 | 54.6 | 1.18 | 0.494 | 36.9 | 0.229 | 11.00 |
| | 3 | 0.396 | 60.3 | 0.798 | 56.8 | 1.18 | 0.494 | 37.0 | 0.229 | 10.46 |
| | 4 | 0.396 | 59.7 | 0.785 | 57.1 | 1.15 | 0.464 | 32.0 | 0.229 | 9.03 |
| | 5 | 0.396 | 59.2 | 0.772 | 39.8 | 1.10 | 0.377 | 33.8 | 0.181 | 8.24 |

TABLE IV-1 (Continued)

| | | | | | | | | | | | | | | | | |
|-------------------|------|------|-------|---|-----|-----|-----|-----|-----|-----|------|-----|-----|-----|-----|-----|
| Axial Distance, d | -2.0 | -1.0 | -0.25 | 0 | 0.1 | 0.3 | 0.5 | 0.7 | 0.9 | 1.1 | 1.35 | 1.6 | 2.1 | 2.6 | 3.1 | 4.1 |
|-------------------|------|------|-------|---|-----|-----|-----|-----|-----|-----|------|-----|-----|-----|-----|-----|

100% N

RATIO OF WALL STATIC PRESSURE TO INLET TOTAL PRESSURE

| | | | | | | | | | | | | | | | | | |
|---------------|-----|-------|-------|-------|-------|-------|-------|-------|-------|-------|-------|-------|-------|-------|-------|-------|-------|
| Maximum RP | O W | 0.846 | 0.832 | 0.806 | 0.690 | 0.627 | 0.758 | 0.826 | 0.968 | 1.082 | 1.181 | 1.246 | 1.240 | 1.242 | 1.296 | 1.377 | 1.438 |
| | I W | 0.840 | | 0.809 | | | | | | | | | 1.164 | 1.263 | | 1.317 | |
| Mean RP | O W | 0.846 | 0.833 | 0.806 | 0.681 | 0.597 | 0.566 | 0.602 | 0.706 | 0.796 | 0.919 | 1.042 | 1.088 | 1.138 | 1.220 | 1.255 | 1.287 |
| | I W | 0.842 | | 0.811 | | | | | | | | | 0.988 | 1.114 | | 1.216 | |
| Minimum RP | O W | 0.828 | 0.813 | 0.788 | 0.658 | 0.587 | 0.556 | 0.524 | 0.502 | 0.535 | 0.620 | 0.676 | 0.704 | 0.734 | 0.811 | 0.834 | 0.947 |
| | I W | 0.823 | 0.813 | 0.788 | | | | | | | | | 0.589 | 0.824 | 0.819 | 0.853 | 0.914 |

90% N

| | | | | | | | | | | | | | | | | | |
|---------------|-----|-------|-------|-------|-------|-------|-------|-------|-------|-------|-------|-------|-------|-------|-------|-------|-------|
| Maximum RP | O W | 0.839 | 0.832 | 0.817 | 0.805 | 0.842 | 0.912 | 1.065 | 1.153 | 1.213 | 1.265 | 1.279 | 1.293 | 1.324 | 1.446 | 1.417 | 1.431 |
| | I W | 0.836 | 0.825 | 0.803 | | | | | | | | | 1.210 | 1.294 | 1.321 | 1.351 | 1.361 |
| Mean RP | O W | 0.828 | 0.820 | 0.795 | 0.698 | 0.651 | 0.731 | 0.777 | 0.812 | 0.976 | 1.066 | 1.160 | 1.180 | 1.212 | 1.332 | 1.306 | 1.325 |
| | I W | 0.828 | 0.819 | 0.796 | | | | | | | | | 1.096 | 1.209 | 1.223 | 1.260 | 1.270 |
| Minimum RP | O W | 0.834 | 0.825 | 0.796 | 0.699 | 0.641 | 0.649 | 0.554 | 0.547 | 0.539 | 0.601 | 0.714 | 0.731 | 0.749 | 0.797 | 0.872 | 0.947 |
| | I W | 0.829 | 0.819 | 0.802 | | | | | | | | | 0.632 | 0.814 | 0.835 | 0.882 | 0.914 |

80% N

| | | | | | | | | | | | | | | | | | |
|---------------|-----|-------|-------|-------|-------|-------|-------|-------|-------|-------|-------|-------|-------|-------|-------|-------|-------|
| Maximum RP | O W | 0.858 | 0.852 | 0.841 | 0.852 | 0.869 | 0.949 | 1.079 | 1.158 | 1.209 | 1.248 | 1.285 | 1.312 | 1.346 | 1.373 | 1.373 | 1.398 |
| | I W | 0.855 | 0.843 | 0.821 | | | | | | | | | 1.212 | 1.280 | | 1.326 | |
| Mean RP | O W | 0.841 | 0.832 | 0.808 | 0.723 | 0.700 | 0.695 | 0.637 | 0.677 | 0.771 | 0.829 | 0.950 | 0.987 | 1.065 | 1.113 | 1.127 | 1.139 |
| | I W | 0.836 | 0.827 | 0.808 | | | | | | | | | 0.930 | 1.051 | 1.068 | 1.096 | 1.099 |
| Minimum RP | O W | 0.845 | 0.837 | 0.810 | 0.751 | 0.704 | 0.701 | 0.629 | 0.591 | 0.586 | 0.653 | 0.766 | 0.824 | 0.928 | 0.966 | 0.975 | 0.980 |
| | I W | 0.839 | 0.828 | 0.810 | | | | | | | | | 0.763 | 0.895 | 0.939 | 0.967 | 0.964 |

I W Inside Wall
O W Outside Wall

54

TABLE IV-1 (Concluded)

| Axial Distance, d | -2.0 | -1.0 | -0.25 | 0 | 0.1 | 0.3 | 0.5 | 0.7 | 0.9 | 1.1 | 1.35 | 1.6 | 2.1 | 2.6 | 3.1 | 4.1 | |
|---|------|-------|-------|-------|-------|-------|-------|-------|-------|-------|-------|-------|-------|-------|-------|-------|-------|
| 70% N | | | | | | | | | | | | | | | | | |
| RATIO OF WALL STATIC PRESSURE TO INLET TOTAL PRESSURE | | | | | | | | | | | | | | | | | |
| Maximum RP | 0 W | 0.889 | 0.888 | 0.885 | 0.897 | 0.906 | 1.002 | 1.099 | 1.156 | 1.185 | 1.210 | 1.247 | 1.272 | 1.287 | 1.352 | 1.309 | 1.304 |
| | 1 W | 0.891 | 0.885 | 0.863 | | | | | | | | | 1.194 | 1.239 | 1.270 | 1.272 | 1.270 |
| Mean RP | 0 W | 0.862 | 0.855 | 0.833 | 0.784 | 0.810 | 0.855 | 0.878 | 0.930 | 0.993 | 1.021 | 1.073 | 1.106 | 1.158 | 1.179 | 1.186 | 1.189 |
| | 1 W | 0.860 | 0.853 | 0.836 | | | | | | | | | 1.054 | 1.128 | 1.141 | 1.160 | 1.160 |
| Minimum RP | 0 W | 0.865 | 0.856 | 0.834 | 0.789 | 0.761 | 0.706 | 0.635 | 0.601 | 0.659 | 0.752 | 0.842 | 0.904 | | | 1.018 | |
| | 1 W | 0.859 | 0.850 | 0.837 | | | | | | | | | 0.872 | 0.966 | | 1.001 | |
| 60% N | | | | | | | | | | | | | | | | | |
| Maximum RP | 0 W | 0.918 | 0.915 | 0.915 | 0.921 | 0.924 | 0.998 | 1.073 | 1.106 | 1.122 | 1.141 | 1.174 | 1.193 | 1.210 | 1.219 | 1.210 | 1.231 |
| | 1 W | 0.918 | 0.914 | 0.906 | | | | | | | | | 1.144 | | | 1.188 | |
| Mean RP | 0 W | 0.903 | 0.898 | 0.891 | 0.883 | 0.906 | 0.929 | 0.949 | 0.964 | 0.986 | 1.008 | 1.046 | 1.063 | 1.109 | 1.123 | 1.136 | 1.126 |
| | 1 W | 0.902 | 0.898 | 0.886 | | | | | | | | | 1.018 | 1.079 | | 1.114 | |
| Minimum RP | 0 W | 0.887 | 0.880 | 0.868 | 0.827 | 0.806 | 0.646 | 0.644 | 0.740 | 0.790 | 0.814 | 0.888 | 0.915 | | | 0.995 | |
| | 1 W | 0.883 | 0.876 | 0.867 | | | | | | | | | 0.903 | 0.956 | | 0.983 | |
| 50% N | | | | | | | | | | | | | | | | | |
| Maximum RP | 0 W | 0.942 | 0.940 | 0.942 | 0.952 | 0.952 | 0.984 | 1.038 | 1.062 | 1.072 | 1.086 | 1.103 | 1.114 | 1.126 | 1.132 | 1.130 | 1.153 |
| | 1 W | 0.942 | 0.940 | 0.931 | | | | | | | | | 1.085 | 1.111 | 1.121 | 1.120 | 1.125 |
| Mean RP | 0 W | 0.923 | 0.916 | 0.914 | 0.916 | 0.923 | 0.948 | 0.971 | 0.982 | 0.986 | 0.993 | 1.028 | 1.052 | | | 1.081 | |
| | 1 W | 0.920 | 0.915 | | | | | | | | | | 1.019 | | | 1.075 | |
| Minimum RP | 0 W | 0.909 | 0.904 | 0.897 | 0.879 | 0.862 | 0.855 | 0.861 | 0.870 | 0.872 | 0.876 | 0.933 | 0.944 | | | 1.002 | |
| | 1 W | 0.910 | 0.905 | 0.898 | | | | | | | | | 0.936 | 0.976 | | 0.992 | |

97

TABLE IV-2
CONFIGURATION 2

| RP | Area Centers | M_2 | β_2 deg | M_{w2} | $\eta\%$ | RP | M_3 | α_3 deg | $G_3 \frac{\sqrt{\theta}}{\delta}$ | $\Delta H/\theta$ |
|---------|--------------|-------|---------------|----------|----------|------|-------|----------------|------------------------------------|-------------------|
| 100% N | | | | | | | | | | |
| MAXIMUM | 1 | 0.583 | 68.2 | 1.569 | 47.0 | 2.07 | 0.748 | 85.0 | 0.048 | 61.21 |
| | 2 | 0.587 | 67.7 | 1.548 | 49.5 | 2.14 | 0.800 | 70.5 | 0.194 | 61.06 |
| | 3 | 0.581 | 67.4 | 1.515 | 56.2 | 2.32 | 0.891 | 55.8 | 0.364 | 60.00 |
| | 4 | 0.575 | 67.2 | 1.482 | 60.1 | 2.41 | 0.944 | 51.0 | 0.429 | 59.16 |
| | 5 | 0.571 | 66.8 | 1.447 | 59.2 | 2.33 | 0.929 | 52.0 | 0.407 | 57.40 |
| MEAN | 1 | 0.594 | 67.9 | 1.577 | 40.9 | 1.75 | 0.726 | 68.6 | 0.171 | 52.89 |
| | 2 | 0.594 | 67.5 | 1.554 | 45.4 | 1.87 | 0.809 | 53.5 | 0.309 | 53.82 |
| | 3 | 0.586 | 67.3 | 1.520 | 47.6 | 1.91 | 0.843 | 50.5 | 0.342 | 53.14 |
| | 4 | 0.578 | 67.1 | 1.485 | 46.4 | 1.83 | 0.814 | 51.2 | 0.322 | 50.38 |
| | 5 | 0.571 | 66.8 | 1.448 | 46.1 | 1.78 | 0.805 | 53.0 | 0.302 | 48.56 |
| MINIMUM | 1 | 0.594 | 68.0 | 1.588 | 9.2 | 1.09 | 0.471 | 63.0 | 0.098 | 34.11 |
| | 2 | 0.598 | 67.6 | 1.566 | 30.4 | 1.41 | 0.882 | 36.4 | 0.337 | 38.93 |
| | 3 | 0.592 | 67.3 | 1.533 | 41.5 | 1.57 | 0.981 | 34.2 | 0.389 | 39.83 |
| | 4 | 0.586 | 67.0 | 1.499 | 34.1 | 1.42 | 0.892 | 35.4 | 0.343 | 38.83 |
| | 5 | 0.581 | 66.6 | 1.463 | 29.7 | 1.34 | 0.842 | 34.0 | 0.328 | 36.16 |
| 90% N | | | | | | | | | | |
| MAXIMUM | 1 | 0.563 | 66.9 | 1.432 | 52.6 | 1.93 | 0.706 | 71.8 | 0.161 | 48.78 |
| | 2 | 0.568 | 66.3 | 1.411 | 56.1 | 1.97 | 0.746 | 64.5 | 0.233 | 47.49 |
| | 3 | 0.562 | 66.0 | 1.383 | 63.7 | 2.10 | 0.824 | 57.4 | 0.323 | 46.14 |
| | 4 | 0.558 | 65.7 | 1.354 | 66.7 | 2.15 | 0.859 | 53.6 | 0.368 | 45.52 |
| | 5 | 0.553 | 65.3 | 1.324 | 65.3 | 2.06 | 0.833 | 54.0 | 0.349 | 43.66 |
| MEAN | 1 | 0.576 | 66.4 | 1.440 | 42.9 | 1.59 | 0.686 | 66.7 | 0.170 | 41.30 |
| | 2 | 0.580 | 65.8 | 1.418 | 49.5 | 1.73 | 0.784 | 52.7 | 0.297 | 42.41 |
| | 3 | 0.573 | 65.6 | 1.388 | 54.1 | 1.78 | 0.827 | 48.0 | 0.345 | 41.14 |
| | 4 | 0.568 | 65.3 | 1.359 | 52.3 | 1.69 | 0.791 | 46.8 | 0.334 | 38.65 |
| | 5 | 0.561 | 65.0 | 1.327 | 50.1 | 1.63 | 0.763 | 50.3 | 0.297 | 37.14 |
| MINIMUM | 1 | 0.575 | 66.4 | 1.440 | 25.7 | 1.24 | 0.620 | 52.6 | 0.199 | 30.43 |
| | 2 | 0.581 | 65.8 | 1.419 | 40.3 | 1.41 | 0.774 | 36.7 | 0.330 | 31.84 |
| | 3 | 0.577 | 65.5 | 1.391 | 37.5 | 1.36 | 0.741 | 37.0 | 0.313 | 30.20 |
| | 4 | 0.572 | 65.1 | 1.362 | 38.5 | 1.35 | 0.741 | 36.0 | 0.316 | 28.66 |
| | 5 | 0.567 | 64.9 | 1.331 | 36.8 | 1.32 | 0.730 | 39.9 | 0.293 | 28.14 |

TABLE IV-2 (Continued)

| RP | Area Centers | M ₂ | β ₂ deg | M _{w2} | η% | RP | M ₃ | α ₃ deg | G ₃ $\frac{\sqrt{\theta}}{\delta}$ | ΔH/θ |
|----|--------------|----------------|--------------------|-----------------|----|----|----------------|--------------------|---|------|
|----|--------------|----------------|--------------------|-----------------|----|----|----------------|--------------------|---|------|

80% N

| | | | | | | | | | | |
|---------|---|-------|------|-------|------|------|-------|------|-------|-------|
| MAXIMUM | 1 | 0.555 | 64.7 | 1.297 | 57.5 | 1.77 | 0.646 | 66.7 | 0.184 | 38.13 |
| | 2 | 0.559 | 64.1 | 1.280 | 62.1 | 1.83 | 0.702 | 61.5 | 0.241 | 37.81 |
| | 3 | 0.555 | 63.8 | 1.255 | 68.0 | 1.91 | 0.762 | 55.4 | 0.310 | 37.22 |
| | 4 | 0.549 | 63.4 | 1.228 | 69.5 | 1.89 | 0.762 | 51.8 | 0.335 | 35.67 |
| | 5 | 0.544 | 63.1 | 1.201 | 67.2 | 1.81 | 0.730 | 53.5 | 0.305 | 34.21 |
| MEAN | 1 | 0.564 | 64.3 | 1.301 | 48.7 | 1.54 | 0.638 | 64.4 | 0.177 | 33.35 |
| | 2 | 0.567 | 63.8 | 1.283 | 54.5 | 1.63 | 0.716 | 51.0 | 0.288 | 34.02 |
| | 3 | 0.563 | 63.4 | 1.258 | 57.6 | 1.64 | 0.737 | 48.0 | 0.314 | 32.83 |
| | 4 | 0.570 | 63.1 | 1.231 | 56.9 | 1.58 | 0.711 | 45.7 | 0.313 | 30.73 |
| | 5 | 0.552 | 62.7 | 1.204 | 54.3 | 1.54 | 0.694 | 49.2 | 0.283 | 30.18 |
| MINIMUM | 1 | 0.561 | 64.4 | 1.300 | 32.4 | 1.26 | 0.598 | 51.6 | 0.205 | 26.55 |
| | 2 | 0.567 | 63.8 | 1.284 | 40.2 | 1.36 | 0.691 | 40.0 | 0.293 | 28.06 |
| | 3 | 0.564 | 63.4 | 1.259 | 40.6 | 1.34 | 0.686 | 39.5 | 0.292 | 26.60 |
| | 4 | 0.559 | 63.0 | 1.233 | 42.7 | 1.32 | 0.683 | 37.0 | 0.300 | 24.28 |
| | 5 | 0.555 | 62.6 | 1.206 | 39.8 | 1.29 | 0.666 | 39.6 | 0.280 | 23.84 |

70% N

| | | | | | | | | | | |
|---------|---|-------|------|-------|------|------|-------|------|-------|-------|
| MAXIMUM | 1 | 0.469 | 65.2 | 1.118 | 64.1 | 1.64 | 0.605 | 65.3 | 0.179 | 29.59 |
| | 2 | 0.489 | 63.9 | 1.112 | 70.0 | 1.69 | 0.654 | 58.7 | 0.240 | 28.87 |
| | 3 | 0.492 | 63.3 | 1.093 | 76.6 | 1.73 | 0.691 | 53.2 | 0.293 | 27.58 |
| | 4 | 0.493 | 62.7 | 1.074 | 79.5 | 1.72 | 0.691 | 50.4 | 0.310 | 26.05 |
| | 5 | 0.495 | 62.0 | 1.056 | 72.4 | 1.60 | 0.623 | 54.5 | 0.251 | 24.72 |
| MEAN | 1 | 0.512 | 63.4 | 1.144 | 52.2 | 1.44 | 0.593 | 59.3 | 0.192 | 26.36 |
| | 2 | 0.527 | 62.3 | 1.135 | 58.3 | 1.50 | 0.650 | 50.6 | 0.261 | 26.12 |
| | 3 | 0.525 | 61.9 | 1.114 | 61.9 | 1.50 | 0.658 | 45.3 | 0.293 | 24.51 |
| | 4 | 0.522 | 61.5 | 1.092 | 61.8 | 1.46 | 0.643 | 43.0 | 0.296 | 23.11 |
| | 5 | 0.519 | 61.0 | 1.070 | 53.6 | 1.37 | 0.576 | 47.6 | 0.241 | 22.08 |
| MINIMUM | 1 | 0.511 | 63.4 | 1.141 | 37.2 | 1.24 | 0.570 | 47.2 | 0.218 | 21.15 |
| | 2 | 0.526 | 62.3 | 1.132 | 44.2 | 1.31 | 0.644 | 41.0 | 0.273 | 22.28 |
| | 3 | 0.525 | 61.8 | 1.112 | 46.2 | 1.31 | 0.655 | 40.0 | 0.281 | 21.48 |
| | 4 | 0.524 | 61.3 | 1.091 | 47.3 | 1.28 | 0.637 | 36.0 | 0.289 | 19.25 |
| | 5 | 0.521 | 60.8 | 1.070 | 39.4 | 1.22 | 0.584 | 39.0 | 0.251 | 18.31 |

TABLE IV-2 (Continued)

| RP | Area Centers | M_2 | β_2 deg | M_{W2} | $\eta\%$ | RP | M_3 | α_3 deg | $G_3 \frac{\sqrt{\theta}}{\delta}$ | $\Delta H/\theta$ |
|----|--------------|-------|---------------|----------|----------|----|-------|----------------|------------------------------------|-------------------|
|----|--------------|-------|---------------|----------|----------|----|-------|----------------|------------------------------------|-------------------|

60% N

| | | | | | | | | | | |
|---------|---|-------|------|-------|------|------|-------|------|-------|-------|
| MAXIMUM | 1 | 0.397 | 65.4 | 0.952 | 68.4 | 1.48 | 0.535 | 63.0 | 0.166 | 21.40 |
| | 2 | 0.412 | 64.2 | 0.945 | 74.7 | 1.52 | 0.582 | 55.8 | 0.224 | 21.08 |
| | 3 | 0.415 | 63.5 | 0.929 | 81.6 | 1.54 | 0.606 | 51.0 | 0.261 | 19.87 |
| | 4 | 0.418 | 62.8 | 0.914 | 83.0 | 1.51 | 0.595 | 48.5 | 0.268 | 18.75 |
| | 5 | 0.422 | 62.0 | 0.898 | 78.7 | 1.46 | 0.559 | 54.0 | 0.222 | 18.04 |
| MEAN | 1 | 0.463 | 62.0 | 0.985 | 55.8 | 1.33 | 0.523 | 56.0 | 0.184 | 19.00 |
| | 2 | 0.470 | 61.2 | 0.975 | 64.7 | 1.38 | 0.582 | 45.3 | 0.257 | 18.59 |
| | 3 | 0.466 | 60.8 | 0.955 | 68.9 | 1.39 | 0.593 | 42.0 | 0.277 | 17.61 |
| | 4 | 0.464 | 60.3 | 0.938 | 69.8 | 1.37 | 0.587 | 40.5 | 0.279 | 16.83 |
| | 5 | 0.462 | 59.9 | 0.919 | 64.7 | 1.33 | 0.550 | 47.0 | 0.233 | 16.13 |
| MINIMUM | 1 | 0.461 | 62.1 | 0.985 | 41.2 | 1.20 | 0.503 | 48.6 | 0.192 | 15.92 |
| | 2 | 0.472 | 61.1 | 0.977 | 50.8 | 1.25 | 0.574 | 39.8 | 0.255 | 16.33 |
| | 3 | 0.470 | 60.7 | 0.959 | 53.1 | 1.25 | 0.580 | 37.5 | 0.266 | 15.61 |
| | 4 | 0.468 | 60.2 | 0.941 | 52.9 | 1.24 | 0.571 | 34.6 | 0.270 | 14.83 |
| | 5 | 0.466 | 59.7 | 0.923 | 50.4 | 1.21 | 0.550 | 40.5 | 0.240 | 14.04 |

50% N

| | | | | | | | | | | |
|---------|---|-------|------|-------|------|------|-------|------|-------|-------|
| MAXIMUM | 1 | 0.317 | 66.4 | 0.790 | 70.0 | 1.32 | 0.460 | 63.3 | 0.135 | 14.64 |
| | 2 | 0.329 | 65.1 | 0.782 | 76.5 | 1.34 | 0.497 | 55.5 | 0.184 | 14.34 |
| | 3 | 0.335 | 64.3 | 0.771 | 82.7 | 1.35 | 0.514 | 51.3 | 0.210 | 13.54 |
| | 4 | 0.339 | 63.5 | 0.758 | 82.9 | 1.33 | 0.499 | 48.6 | 0.215 | 12.80 |
| | 5 | 0.342 | 62.7 | 0.745 | 78.2 | 1.30 | 0.465 | 51.4 | 0.188 | 12.25 |
| MEAN | 1 | 0.403 | 61.0 | 0.831 | 62.2 | 1.23 | 0.457 | 48.0 | 0.189 | 12.36 |
| | 2 | 0.412 | 60.0 | 0.824 | 68.9 | 1.26 | 0.501 | 42.6 | 0.228 | 12.48 |
| | 3 | 0.412 | 59.4 | 0.810 | 72.3 | 1.27 | 0.511 | 40.2 | 0.241 | 12.02 |
| | 4 | 0.410 | 59.0 | 0.795 | 72.7 | 1.25 | 0.500 | 38.6 | 0.240 | 11.34 |
| | 5 | 0.408 | 58.5 | 0.780 | 68.0 | 1.22 | 0.464 | 46.0 | 0.197 | 10.56 |
| MINIMUM | 1 | 0.417 | 60.2 | 0.838 | 44.9 | 1.15 | 0.445 | 45.4 | 0.182 | 11.23 |
| | 2 | 0.424 | 59.3 | 0.830 | 54.5 | 1.19 | 0.500 | 36.2 | 0.235 | 11.38 |
| | 3 | 0.423 | 58.8 | 0.815 | 58.5 | 1.19 | 0.512 | 35.6 | 0.242 | 10.88 |
| | 4 | 0.421 | 58.3 | 0.801 | 59.7 | 1.18 | 0.509 | 34.6 | 0.243 | 10.29 |
| | 5 | 0.417 | 57.9 | 0.784 | 51.1 | 1.15 | 0.464 | 40.5 | 0.204 | 9.59 |

TABLE IV-2 (Continued)

| Axial Distance, d | -2.0 | -1.0 | -0.25 | 0 | 0.1 | 0.3 | 0.5 | 0.7 | 0.9 | 1.1 | 1.35 | 1.6 | 2:1 | 2.6 | 3.1 | 4.1 | |
|--|------|-------|-------|-------|-------|-------|-------|-------|-------|-------|-------|-------|-------|-------|-------|-------|-------|
| 100% N RATIO OF WALL STATIC PRESSURE TO INLET TOTAL PRESSURE | | | | | | | | | | | | | | | | | |
| Maximum RP | O W | 0.828 | 0.814 | 0.789 | 0.699 | 0.712 | 0.872 | 1.076 | 1.101 | 1.270 | 1.298 | 1.274 | 1.275 | 1.301 | 1.361 | 1.445 | 1.489 |
| | I W | 0.825 | 0.818 | 0.804 | | | | | | | | 1.143 | 1.238 | 1.270 | 1.273 | 1.325 | 1.361 |
| Mean RP | O W | 0.824 | 0.811 | 0.784 | 0.684 | 0.544 | 0.514 | 0.554 | 0.687 | 0.884 | 0.978 | 1.002 | 1.049 | 1.116 | 1.198 | 1.246 | 1.257 |
| | I W | 0.823 | 0.816 | 0.803 | | | | | | | | 0.890 | 0.987 | 1.122 | 1.130 | 1.157 | 1.177 |
| Minimum RP | O W | 0.825 | 0.810 | 0.783 | 0.687 | 0.544 | 0.502 | 0.442 | 0.402 | 0.425 | 0.596 | 0.666 | 0.667 | 0.726 | 0.813 | 0.857 | 0.936 |
| | I W | 0.824 | 0.814 | 0.796 | | | | | | | | 0.548 | 0.606 | 0.806 | 0.806 | 0.841 | 0.904 |
| 90% N | | | | | | | | | | | | | | | | | |
| Maximum RP | O W | 0.829 | 0.823 | 0.801 | 0.743 | 0.764 | 0.872 | 1.063 | 1.086 | 1.167 | 1.261 | 1.277 | 1.280 | 1.289 | 1.361 | 1.395 | 1.412 |
| | I W | 0.841 | 0.831 | 0.815 | | | | | | | | 1.169 | 1.221 | 1.269 | 1.266 | 1.299 | 1.316 |
| Mean RP | O W | 0.824 | 0.820 | 0.793 | 0.713 | 0.591 | 0.612 | 0.532 | 0.675 | 0.837 | 0.931 | 1.015 | 1.036 | 1.049 | 1.132 | 1.173 | 1.194 |
| | I W | 0.831 | 0.822 | 0.810 | | | | | | | | 0.911 | 0.980 | 1.077 | 1.076 | 1.101 | 1.126 |
| Minimum RP | O W | 0.825 | 0.819 | 0.793 | 0.717 | 0.593 | 0.607 | 0.473 | 0.455 | 0.522 | 0.662 | 0.748 | 0.771 | 0.826 | 0.921 | 0.960 | 0.981 |
| | I W | 0.832 | 0.823 | 0.806 | | | | | | | | 0.683 | 0.740 | 0.885 | 0.898 | 0.926 | 0.945 |
| 80% N | | | | | | | | | | | | | | | | | |
| Maximum RP | O W | 0.840 | 0.829 | 0.807 | 0.751 | 0.766 | 0.857 | 0.896 | 1.019 | 1.083 | 1.177 | 1.246 | 1.252 | 1.270 | 1.320 | 1.343 | 1.345 |
| | I W | 0.846 | 0.837 | 0.819 | | | | | | | | 1.152 | 1.204 | 1.250 | 1.242 | 1.263 | 1.280 |
| Mean RP | O W | 0.836 | 0.828 | 0.802 | 0.739 | 0.651 | 0.648 | 0.578 | 0.710 | 0.836 | 0.927 | 1.029 | 1.065 | 1.090 | 1.158 | 1.176 | 1.175 |
| | I W | 0.839 | 0.829 | 0.814 | | | | | | | | 0.957 | 1.015 | 1.100 | 1.096 | 1.112 | 1.127 |
| Minimum RP | O W | 0.838 | 0.827 | 0.803 | 0.742 | 0.652 | 0.641 | 0.489 | 0.499 | 0.580 | 0.709 | 0.782 | 0.809 | 0.896 | 0.972 | 0.998 | 0.990 |
| | I W | 0.838 | 0.830 | 0.812 | | | | | | | | 0.751 | 0.813 | 0.919 | 0.934 | 0.990 | 0.964 |

50

TABLE IV-2 (Concluded)

| Axial Distance, d | -2.0 | -1.0 | -0.25 | 0 | 0.1 | 0.3 | 0.5 | 0.7 | 0.9 | 1.1 | 1.35 | 1.6 | 2.1 | 2.6 | 3.1 | 4.1 |
|-------------------|------|------|-------|---|-----|-----|-----|-----|-----|-----|------|-----|-----|-----|-----|-----|
|-------------------|------|------|-------|---|-----|-----|-----|-----|-----|-----|------|-----|-----|-----|-----|-----|

70% N

| | | | | | | | | | | | | | | | | | |
|---------------|-----|-------|-------|-------|-------|-------|-------|-------|-------|-------|-------|-------|-------|-------|-------|-------|-------|
| Maximum RP | 0 W | 0.870 | 0.862 | 0.853 | 0.842 | 0.875 | 0.947 | 1.060 | 1.081 | 1.124 | 1.183 | 1.217 | 1.234 | 1.251 | 1.280 | 1.291 | 1.296 |
| | 1 W | 0.876 | 0.870 | 0.846 | | | | | | | | 1.137 | 1.176 | 1.218 | 1.224 | 1.227 | 1.240 |
| Mean RP | 0 W | 0.859 | 0.849 | 0.828 | 0.785 | 0.721 | 0.669 | 0.644 | 0.723 | 0.854 | 0.957 | 1.027 | 1.077 | 1.111 | 1.132 | 1.144 | 1.142 |
| | 1 W | 0.857 | 0.851 | 0.834 | | | | | | | | 0.976 | 1.019 | 1.087 | 1.096 | 1.093 | 1.100 |
| Minimum RP | 0 W | 0.859 | 0.849 | 0.829 | 0.784 | 0.720 | 0.657 | 0.517 | 0.536 | 0.686 | 0.761 | 0.819 | 0.868 | 0.948 | 0.983 | 0.998 | 0.996 |
| | 1 W | 0.859 | 0.851 | 0.833 | | | | | | | | 0.809 | 0.858 | 0.917 | 0.961 | 0.964 | 0.967 |

60% N

| | | | | | | | | | | | | | | | | | |
|---------------|-----|-------|-------|-------|-------|-------|-------|-------|-------|-------|-------|-------|-------|-------|-------|-------|-------|
| Maximum RP | 0 W | 0.899 | 0.896 | 0.894 | 0.899 | 0.911 | 0.967 | 1.045 | 1.065 | 1.096 | 1.137 | 1.168 | 1.188 | 1.192 | 1.214 | 1.220 | 1.217 |
| | 1 W | 0.904 | 0.902 | 0.885 | | | | | | | | 1.112 | 1.132 | 1.175 | 1.167 | 1.176 | 1.182 |
| Mean RP | 0 W | 0.877 | 0.874 | 0.859 | 0.820 | 0.762 | 0.655 | 0.734 | 0.818 | 0.874 | 0.967 | 1.033 | 1.065 | 1.081 | 1.103 | 1.109 | 1.100 |
| | 1 W | 0.879 | 0.875 | 0.866 | | | | | | | | 0.995 | 1.024 | 1.068 | 1.066 | 1.016 | 1.070 |
| Minimum RP | 0 W | 0.880 | 0.874 | 0.859 | 0.819 | 0.759 | 0.606 | 0.541 | 0.684 | 0.786 | 0.826 | 0.883 | 0.938 | 0.979 | 0.997 | 1.010 | 1.006 |
| | 1 W | 0.879 | 0.874 | 0.864 | | | | | | | | 0.878 | 0.919 | 0.977 | 0.982 | 0.986 | 0.984 |

50% N

| | | | | | | | | | | | | | | | | | |
|---------------|-----|-------|-------|-------|-------|-------|-------|-------|-------|-------|-------|-------|-------|-------|-------|-------|-------|
| Maximum RP | 0 W | 0.931 | 0.930 | 0.930 | 0.936 | 0.944 | 0.968 | 1.030 | 1.045 | 1.070 | 1.095 | 1.113 | 1.122 | 1.132 | 1.146 | 1.144 | 1.145 |
| | 1 W | 0.936 | 0.935 | 0.922 | | | | | | | | 1.078 | 1.085 | 1.113 | 1.118 | 1.115 | 1.120 |
| Mean RP | 0 W | 0.903 | 0.899 | 0.889 | 0.867 | 0.821 | 0.842 | 0.868 | 0.899 | 0.927 | 0.973 | 1.029 | 1.047 | 1.064 | 1.075 | 1.072 | 1.070 |
| | 1 W | 0.909 | 0.906 | 0.893 | | | | | | | | 1.004 | 1.017 | 1.045 | 1.054 | 1.048 | 1.052 |
| Minimum RP | 0 W | 0.898 | 0.896 | 0.883 | 0.850 | 0.750 | 0.585 | 0.697 | 0.788 | 0.825 | 0.864 | 0.921 | 0.960 | 0.994 | 1.006 | 1.005 | 1.003 |
| | 1 W | 0.903 | 0.900 | 0.889 | | | | | | | | 0.932 | 0.945 | 0.979 | 0.991 | 0.986 | 0.987 |

51

DOCUMENT CONTROL DATA - R & D

(Security classification of title, body of abstract and indexing annotation must be entered when the overall report is classified)

| | | | |
|---|--|---|--|
| 1. ORIGINATING ACTIVITY (Corporate author) Arnold Engineering Development Center ARO, Inc., Contract Operator Arnold Air Force Station, Tennessee | | 2a. REPORT SECURITY CLASSIFICATION UNCLASSIFIED | |
| | | 2b. GROUP N/A | |
| 3. REPORT TITLE EXPERIMENTAL INVESTIGATION OF TWO BLUNT TRAILING EDGE SUPERSONIC COMPRESSOR ROTORS OF DIFFERENT BLADE THICKNESSES AND WITH CIRCULAR ARC CAMBER LINE | | | |
| 4. DESCRIPTIVE NOTES (Type of report and inclusive dates) | | | |
| 5. AUTHOR(S) (First name, middle initial, last name) C. T. Carman and J. R. Myers, ARO, Inc., and A. J. Wennerstrom and John W. Steurer, Aerospace Research Laboratories | | | |
| 6. REPORT DATE September 1968 | 7a. TOTAL NO. OF PAGES 58 | 7b. NO OF REFS 5 | |
| 8a. CONTRACT OR GRANT NO F40600-69-C-0001 | 9a. ORIGINATOR'S REPORT NUMBER(S) AEDC-TR-68-197 | | |
| b. PROJECT NO 7065 | | | |
| c. Program Element 6144501F | 9b. OTHER REPORT NO(S) (Any other numbers that may be assigned this report) N/A | | |
| d. | | | |
| 10. DISTRIBUTION STATEMENT This document has been approved for public release and sale; its distribution is unlimited. | | | |
| 11. SUPPLEMENTARY NOTES Available in DDC. | | 12. SPONSORING MILITARY ACTIVITY Arnold Engineering Development Center, Air Force Systems Command, Arnold Air Force Station, Tennessee | |
| 13. ABSTRACT Two configurations of blunt-trailing-edge supersonic compressor blades were tested with air in the AEDC compressor rig. The performance of these blades was investigated over the speed range from 50 to 100 percent of design speed. The performance of the two blade configurations is compared, and the effect of the modifications between the two configurations is evaluated. | | | |

| 14 | KEY WORDS | LINK A | | LINK B | | LINK C | |
|----|---|--------|----|--------|----|--------|----|
| | | ROLE | WT | ROLE | WT | ROLE | WT |
| | supersonic compressors compressor rotors compressor blades blunt trailing edge performance pressure distribution Mach number distribution | | | | | | |
| | 1. Rotors -- Trailing edges | | | | | | |
| | 2 Blades -- " | | | | | | |
| | 3 Blades -- Pressure distribution | | | | | | |
| | 4 " -- Mach Velocity distribution | | | | | | |